ON MAGNON SUPERFLUIDITY IN FERROMAGNETIC FILMS

A Dissertation

by

CHEN SUN

Submitted to the Office of Graduate and Professional Studies of
Texas A&M University
in partial fulfillment of the requirements for the degree of

DOCTOR OF PHILOSOPHY

Chair of Committee,	Valery L. Pokrovsky
Committee Members,	Artem G. Abanov
	Wenhao Wu
	Gregory Berkolaiko
Head of Department,	Grigory V. Rogachev

August 2018

Major Subject: Physics

ABSTRACT

More than ten years ago, Bose-Einstein condensation (BEC) of magnons (or quantized spin waves) was experimentally observed in yttrium iron garnet (YIG) films at room temperature. Since BEC and superfluidity are closely related phenomena, it is natural to ask whether such magnon condensates can transport as superfluid and, if so, how such superfluid looks like. In this work, we study theoretically superfluidity of magnons in ferromagnetic films. We first give an review of the basic theory of magnons in ferromagnetic films. We then discuss BEC of magnons from both experimental and theoretical points of view. Then we study superfluidity of magnons in ferromagnetic films by starting from a model of spins in ferromagnetic films. Model in terms of magnon operators is then introduced, and a Hamiltonian describing the condensed magnons is derived. Focusing on the one-dimensional (1D) stationary case, we study behaviors of superfluid formed by the condensed magnons. We found an unconventional soliton-like profile of the magnon superfluid, as compared to a uniform superflow, which we argued to be due to the dipolar interaction. We also show by estimates that in YIG films it is possible to have a superfluid current that strongly exceeds the current of normal magnons, so the magnon superfluidity could possibly be observed.

DEDICATION

To my parents.

ACKNOWLEDGMENTS

First I would like to thank my advisor, Professor Valery Pokrovsky for his instructions on this work and for his guidance throughout my PhD. I appreciate him for always being patient to answer my questions and for leading me through the difficulties during research. His enthusiasm for understanding new things has always been impressing and encouraging me. From him I learnt not only knowledge in condensed matter physics, but also ways of doing scientific research, which would continue to benefit me in the future.

I would like to thank my committee members, Professors Artem Abanov, Wenhao Wu and Gregory Berkolaiko, for their suggestions on this work. My thanks also go to Drs. Nikolai Sinitsyn, Wayne Saslow and Thomas Nattermann, by collaborating with and learning from whom I benefited a lot.

I also thank all my friends here. Being at this small town without many ways of entertainments, it is the company of friends that makes my graduate life a wonderful experience. Among them I would give my special thanks to my senior group fellow Fuxiang Li, and my roommate Zhidong Yang.

When I initially chose physics as my major, my parents actually preferred that I chose something else, but finally they supported my decision and kept encouraging me to pursue my dream to become a scientist. During these years when I am far from home, their love is the most valuable thing that supports me and gives me energy. I dedicate this dissertation to them.

CONTRIBUTORS AND FUNDING SOURCES

Contributors

This work was supported by a dissertation committee consisting of Professor Valery L. Pokrovsky (advisor) and Professors Artem G. Abanov and Wenhao Wu of the Department of Physics and Astronomy, and Professor Gregory Berkolaiko of the Department of Mathematics.

This work was carried out by the student under the guidance of Professor Valery L. Pokrovsky, and partially of Dr. Thomas Nattermann from University of Cologne.

Funding Sources

This work was financially supported by research assistantship from my advisor Dr. Valery Pokrovsky under the auspices of 02-512992 William R Thurman '58 Chair Physics, and partially by teaching assistantship from the department of Physics and Astronomy at Texas A&M University.

NOMENCLATURE

BEC	Bose-Einstein condensation
BLS	Brillioun light scattering
EOM	equation of motion
EPM	easy-plane magnet
YIG	yttrium iron garnet
1D	one dimension/one-dimensional
2D	two dimension/two-dimensional
3D	three dimension/three-dimensional

TABLE OF CONTENTS

Page

LIST OF FIGURES

FIGURE Page

1. INTRODUCTION

In 2006, Bose-Einstein condensation (BEC) of magnons (quantized spin waves) was experimentally observed in yttrium iron garnet (YIG) films at room temperature [1]. The magnons are excited by an external ac magnetic field. The pumped magnons have a large lifetime, so that before dissipating their energies to other system (e.g. phonons) and disappearing, they relax among themselves and reach a quasi-equilibrium. Therefore, there exists a chemical potential associated with the magnons, which magnitude is determined by the strength of pumping. When the pumping power exceeds a certain threshold, the chemical potential reaches the gap of the spectrum, and additional magnons aggregate at the bottom of the spectrum, forming a condensate.

The spectrum of magnons in thin ferromagnetic films, when taking into account the dipolar interaction, has two minima [2] Correspondingly, there exist two condensates of magnons. By observing interference patterns of these two condensates [3], the coherence of the condensate wave function was proved, giving a strong support that the magnons indeed develop BECs.

Properties of the magnon BEC in YIG have also been studied theoretically. In [4], it was predicted that, depending on the film thickness and external magnetic field strength, the magnon BEC can develop different states – the symmetric state where the two condensates are populated equally, and the non-symmetric state where they are populated unequally. In general, the symmetric state is more favorable for thinner films. It was also proposed that a new type of oscillation mode called zero-sound exists, which corresponds to modulation of the relative phase and density of the two condensates [4].

Since BEC and superfluidity are closed related, it is natural to ask whether such magnon condensates in YIG can behave like superfluid, and further what are the properties of such magnon superfluid. In this dissertation, we study theoretically superfluidity of magnons in ferromagnetic films, especially in YIG. Since superfluid flow is dissipationless, it can serve as an effective media to transfer information. Thus, this study may have promising applications in the field of magnonics, which investigates information transport and processing by spin waves [5]. The study presented in

this dissertation have been published in [6] and in [7].

The outline of this dissertation is as follows:

In Chapter 2, we review the theory of magnons in ferromagnetic films. We will first give an introduction to the mathematical formulation of spin operators. We then talk about various magnetic interactions, including the exchange interaction, the dipolar interaction and the Zeeman interaction. After that we discuss the model describing magnons in ferromagnetic films. Starting from a Hamiltonian in terms of spin operators, we perform the Holstein-Primakoff transformation to write the Hamiltonian in terms of bosonic operators. After a further Bogoliubov transformation we arrive at a Hamiltonian in terms of magnon operators, from which we could obtain the spectrum of magnons.

In Chapter 3, we discuss Bose-Einstein condensation (BEC) of magnons in ferromagnetic films, especially in the material yttrium iron garnet (YIG). We will start with discussing magnetic properties of the material YIG on which magnon BEC was discovered. We then discuss about the experimental observations of BEC of magnons. It is followed by a discussion on the theory that describing this magnon BEC. We also mention an alternative classical interpretation of the magnon condensate.

In Chapter 4, we consider superfluidity of condensed magnons in YIG. Starting with a Hamiltonian for magnon condensates, we will first derive and examine the equations of motion of the condensate amplitudes, and further for the condensate densities and phases. We then fix to the one-dimensional stationary situation and show by calculations that the superfluidity of condensed magnons is indeed possible, and that such superfluid has a rather unconventional behavior, namely, the superfluid flow is not uniform but soliton-like. We further argue that such a behavior has its origin due to the existence of the dipolar interaction, which breaks the U(1) rotation symmetry of the condensate phase. For the calculations we use a variational method and then an improved numerical shooting method. We also make connections to previous theories of superfluidity in magnetic systems, estimate the relative strength of superfluid and normal currents to show that the magnon superfluidity can indeed manifest itself, and discuss propose possible ways to achieve this

superfluidity experimentally.

At the end of each of the previous three chapters, we discuss several other issues, e.g. on validity of our considerations or approximations, or on some alternative approaches. Those discussions may be "marginal" and skipping them should does not impact the completeness of materials in the chapters, but they could help in clarification.

Finally, in Chapter 5 we present conclusions and discuss open questions.

2. THEORY OF MAGNONS IN FERROMAGNETIC FILMS

Spin waves, introduced by Bloch [8], are collective motion of spins in magnetically ordered media. Their roles in magnetic media is similar to the roles that sound waves play in elastic media. Classically, a spin wave is a precession of magnetization vectors around the equilibrium direction that propagates through some magnetic medium, as illustrated in Fig. 2.1. A magnetic medium that supports spin waves could be ferromagnetic or antiferromagnetic. The equilibrium configuration can be a spontaneously ordered state without any external magnetic field, or, in the ferromagnetic case, it can be set by the direction of an applied magnetic field.

The quantum mechanical version of spin waves, known as magnons, was also introduced by Bloch [8]. Magnons are elementary excitations from a ferromagnetic (or antiferromagnetic) ground state. Qualitative theory for magnons was introduced by Holstein and Primakoff [9] and by Dyson [10]. They showed by using the second quantization formalism that magnons behave as weakly interacting bosonic quasiparticles. As a quasiparticle, a magnon carry certain energy, momentum and spin.

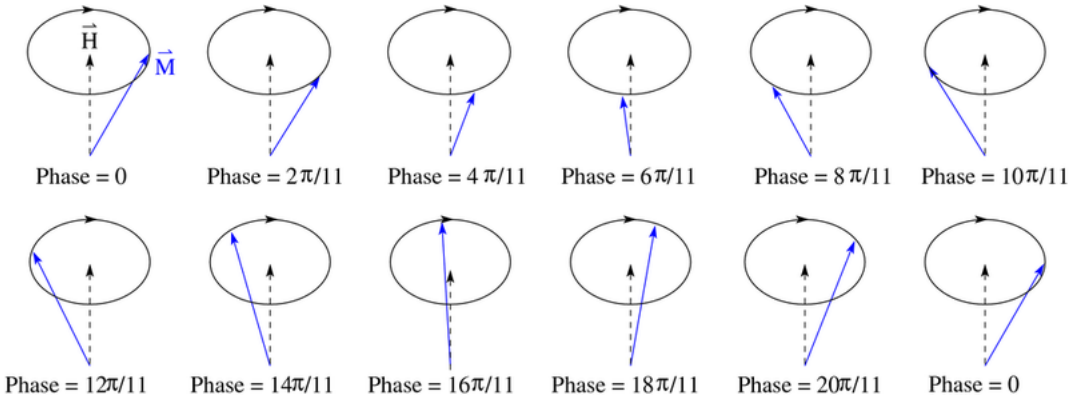

Figure 2.1: Illustration of a spin wave (figure from Wikipedia). Magnetization vectors $\mathbf{M}$ process around their equilibrium direction, which is here determined by the external magnetic field $\mathbf{H}$.

In this chapter, we present an introduction to fundamental theories of magnons in ferromagnets,

focusing on the geometry of films. We will first discuss the mathematical formulation of spin operators, then various magnetic interactions, finally the model describing magnons in ferromagnetic films. This chapter serves as a basis of discussions on BEC and superfluidity of magnons in later chapters.

2.1 Mathematical formulation of quantum spins

In models of magnetic systems, the fundamental objects are spins. We will focus on quantum mechanical models, in which spins are described by spin vector operators $\mathbf{S}_i = (S_i^x, S_i^y, S_i^z)$ defined on lattice sites labelled by the index i. Physically, a spin of a site could originate from localized electrons of the atom on that site. Here we will not worry about the physical nature of spins, but instead just consider them as abstract objects.

The fundamental properties of spin operators are their commutation relations. Spins operators on different sites commute, whereas spin operators on the same site satisfy commutation relations analogous to those of angular momenta:

$$[S_i^\alpha, S_i^\beta] = i\hbar\varepsilon_{\alpha\beta\gamma}S_i^\gamma, \quad \alpha, \beta = x, y, \tag{2.1}$$

where $\varepsilon_{\alpha\beta\gamma}$ is the Levi-Civita symbol, and summation over the repeated index $\gamma = x, y, z$ is assumed. According to quantum mechanics, the component of a spin operator S^α measured along any direction can take a discrete set of values

$$S^\alpha = \hbar s^\alpha, \quad s^\alpha \in \{-s, -(s-1), \ldots, s-1, s\}, \quad \alpha = x, y, z, \tag{2.2}$$

where s is the so-called principal spin quantum number which can take any non-negative half-integer, and s^α is the so-called spin projection quantum number along the α-axis. Note the appearance of $\hbar$, which indicates that the spin operators have the same dimension as an angular momentum. In later discussions, we will take the convention that $\hbar = 1$. The eigenvectors of the

operators $S^2 \equiv (S^x)^2 + (S^y)^2 + (S^z)^2$ and S^z are:

$$S^2|s, m_s\rangle = s(s+1)|s, m_s\rangle, \tag{2.3}$$

$$S^z|s, m_s\rangle = m_s|s, m_s\rangle, \tag{2.4}$$

where $m_s \equiv s^z$ is the spin projection quantum number along the z-axis (also known as the magnetic quantum number).

In many cases it is convenient to introduce the spin raising and lowering operators $S_\pm \equiv S^x \pm iS^y$. Acting them on the eigenvectors $|s, m_s\rangle$, we have:

$$S^\pm|s, m_s\rangle = \sqrt{s(s+1) - m_s(m_s \pm 1)}|s, m_s \pm 1\rangle. \tag{2.5}$$

Namely, acting S^+ or S^- on a state gives another state with a projection higher or lower by 1. The commutation relations in terms of S^z and $S^\pm$ read:

$$[S^z, S^+] = S^+, \tag{2.6}$$

$$[S^z, S^-] = S^-, \tag{2.7}$$

$$[S^+, S^-] = 2S^z. \tag{2.8}$$

2.2 Magnetic interactions

Before discussing the model describing magnons in ferromagnets, we review different kinds of interactions in magnetic materials. Among them are the exchange interaction, the Zeeman interaction, and the dipolar interaction.

2.2.1 Exchange interaction

The exchange interaction is perhaps the most important interaction in magnetic materials. Its origin is completely quantum-mechanical – the wave function of indistinguishable particles has exchange symmetry. Consider a system with two electrons in two atoms (like the situation in a

hydrogen molecule). The Coulomb interaction between the electrons splits the energies of the symmetric and antisymmetric spatial wave functions of the two electrons, so the one with a lower energy is favored. For a system of fermions the overall wave function must be antisymmetric, so for the symmetric/antisymmetric spatial wave function the spin-part of the wave function is antisymmetric/symmetric. This means that a state when the spins of the two electrons are parallel and a state when the spin are antiparallel have different energies. Focusing on the spin variables, we could write an effective interaction proportional to the dot product of the two spins, with a coefficient proportional to the aforementioned energy splitting. For a lattice of spins, this argument leads to the following expression of the exchange interaction, known as the Heisenberg model:

$$H_{ex} = -\sum_{i,j} J_{ij} \mathbf{S}_i \cdot \mathbf{S}_j, \tag{2.9}$$

where J_{ij} is the exchange constant between the sites i and j. An important property of the exchange energy in the form of (2.9) is that, it is invariant under a uniform rotation of every spin (an SO(3) symmetry). This symmetry corresponds to conservation of any component of the total spin of all the sites $S^\alpha_{tot} \equiv \sum_i S^\alpha_i$ ($\alpha = x, y, z$), as can be checked by calculating $[H_{ex}, S^\alpha_{tot}] = 0$ using the commutation relations (2.1).

In practice, models with nonzero couplings J_{ij} only for nearest neighbors are often considered, and the couplings are taken to be uniform, namely,

$$J_{ij} = \begin{cases} J, & \text{if } i, j \text{ are nearest neighbors,} \\ 0, & \text{else.} \end{cases} \tag{2.10}$$

Under these simplifications, the exchange interaction (2.9) becomes:

$$H_{ex} = -J \sum_{\langle i,j \rangle} \mathbf{S}_i \cdot \mathbf{S}_j, \tag{2.11}$$

where $\langle i, j \rangle$ denotes summation over nearest-neighbor sites only. Now we could distinguish

between the two cases of $J > 0$ and $J < 0$. For $J > 0$, the exchange interaction is called ferromagetic, in which case the ground state spin configurations have all spins pointing in the same direction. The ground states are degenerate, due to the aforementioned SO(3) symmetry. For $J < 0$, the exchange interaction is called antiferromagetic. Neighboring spins would favor antiparallel configuration, and the overall spin configuration depends on type of the lattice. For a lattice which can be separated into two interpenetrating sublattices with any site on one sublattice having all nearest neighbors belonging to the other sublattice (e.g. a 2D square lattice), the ground states are such that all spins in each sublattice are in the same direction, and the two sublattices have opposite spin directions. If all spins are of the same amplitudes there will be no net total magnetization. But it may happen that spins on the two sublattices have different magnitudes, in which case there will be a finite net total magnetization. Materials of this kind are known as ferrimagnets. Later in this work, we will focus on the ferromagnetic case.

2.2.2 Zeeman interaction

Zeeman energy describes interaction of spins with an external magnetic field. It takes a simple form:

$$H_Z = -g\mu_B \sum_i \mathbf{S}_i \cdot \mathbf{H}, \tag{2.12}$$

where g is the Landé g-factor, μ_B is the Bohr magneton, and $\mathbf{H}$ is a uniform external magnetic field. The effect of H_Z is to lower the energy of the system when spins are pointing in the same direction of $\mathbf{H}$. It lifts the degeneracy of the ground states when there is only the exchange interaction, so that the ground state is now unique, with all spins pointing in the field direction. The Zeeman interaction breaks the rotational symmetry around any axis not parallel to $\mathbf{H}$, but the rotational symmetry around $\mathbf{H}$ (a U(1) symmetry) is still preserved, and the component of the total spin along the direction of $\mathbf{H}$ is conserved. For example, if $\mathbf{H}$ is along z-axis, then S^z_{tot} is conserved, as one can check that H_Z commutes with S^z_{tot}.

2.2.3 Dipolar interaction

Another important interaction in magnetic systems is the dipolar interaction. Unlike the exchange interaction which arises quantum mechanically, the dipolar interaction can be explained purely classically – it is the direct interaction between two magnetic dipoles. In terms of spin operators, it can be written as:

$$H_d = -\frac{1}{2}(g\mu_B)^2 \sum_{i \neq j} \frac{3(\mathbf{S}_i \cdot \hat{\mathbf{r}}_{ij})(\mathbf{S}_j \cdot \hat{\mathbf{r}}_{ij}) - \mathbf{S}_i \cdot \mathbf{S}_j}{r_{ij}^3}, \tag{2.13}$$

where $\mathbf{r}_{ij} \equiv \mathbf{r}_i - \mathbf{r}_j$ is the vector from the site j to the site i (with $\mathbf{r}_i$ being the position of the site i), and $\hat{\mathbf{r}}_{ij} \equiv \mathbf{r}_{ij}/r_{ij}$ is the unit vector along $\mathbf{r}_{ij}$. The summation is over any lattice sites i and j, but excluding the cases of $i = j$.

Generally, the dipolar interaction is weak as compared to the exchange interaction. But its long-ranged nature indicates that it could play important roles at large scales, or equivalently at small wavevectors. In fact, the dipolar interaction is responsible for the formation of different domains in ferromagets. Another important fact is that the dipolar interaction is not invariant under a uniform rotation of all spins, which is due to the first term in the numerator of (2.13). Correspondingly, no components of the total spin is conserved when the dipolar interaction is included.

2.2.4 Other interactions

The aforementioned three types of interactions will be encountered for later considerations. Besides, there are other interactions, which we will mention briefly here.

The anisotropy energy is another commonly considered type of energy in magnetic systems. It favors magnetization along certain axis or in certain plane. Its origin could be crystalline structures. Besides, for a given shape of material, the dipolar interaction usually causes a certain direction or plane to be preferable, which leads to an effective anisotropy. In fact, in many cases it may be difficult to treat the dipolar interaction directly, and as an approximation this effective anisotropy enters the considered model instead.

Another kind of interaction, the Dzyaloshinsky-Moriya interaction [11, 12], arises only in

materials which lack inversion symmetry. Absence of this symmetry could exist for a crystal structure which is by itself non-centrosymmetric, or it could exist at an interface between two different materials. It favors formations of helical structures and skyrmions.

2.3 Model of magnons in ferromagnetic films

Now we are ready to discuss the model of magnons in ferromagets. Our starting point is a model for a lattice of spins, with a Hamiltonian that includes the nearest-neighbor exchange, Zeeman and dipolar interactions:

$$H = H_{ex} + H_Z + H_d, \tag{2.14}$$

$$H_{ex} = -J \sum_{\langle i,j \rangle} \mathbf{S}_i \cdot \mathbf{S}_j, \tag{2.15}$$

$$H_Z = -g\mu_B H_0 \sum_i S_i^z, \tag{2.16}$$

$$H_d = -\frac{1}{2}(g\mu_B)^2 \sum_{i \neq j} \frac{3(\mathbf{S}_i \cdot \hat{\mathbf{r}}_{ij})(\mathbf{S}_j \cdot \hat{\mathbf{r}}_{ij}) - \mathbf{S}_i \cdot \mathbf{S}_j}{r_{ij}^3}, \tag{2.17}$$

where we have taken the external magnetic field $\mathbf{H}_0$ to be along the $+z$ direction. We assume $J > 0$ so the exchange interaction is ferromagnetic. We will consider the geometry of a film, namely, one of the dimension is much smaller than the other two. In particular, we take the material to be extended in the x and z directions with a large area A, but confined in the y direction with a small thickness d, as sketched in Fig. 2.2. We also take the lattice to be simple cubic with a lattice constant a and three primitive lattice vectors along x, y and z directions, respectively.

2.3.1 Hamiltonian in wavevector space

In our model (2.14), the spins are defined on a lattice. It will be more convenient to work in the wavevector space, which can be achieved by performing a Fourier transformation. Let's define

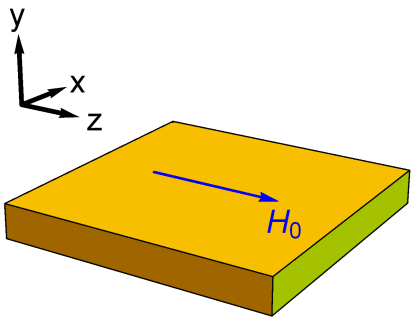

Figure 2.2: Geometry of the considered model. The material is extended in the x and z directions with an area A, and has a thickness d in the y direction. The external magnetic field $\mathbf{H}_0$ is applied in the film plane in the $+z$ direction.

Fourier transformation of the spin vector operators as:

$$\mathbf{S}_i = \frac{1}{\sqrt{N}} \sum_{\mathbf{k}} e^{i\mathbf{k}\cdot\mathbf{r}} \mathbf{S}(\mathbf{k}), \tag{2.18}$$

$$\mathbf{S}(\mathbf{k}) = \frac{1}{\sqrt{N}} \sum_{i} e^{-i\mathbf{k}\cdot\mathbf{r}} \mathbf{S}_i. \tag{2.19}$$

where N is the total number of sites. Similarly, we define Fourier transformation for the spin raising operators $S_i^+ \equiv S_i^x + iS_i^y$:

$$S_i^+ = \frac{1}{\sqrt{N}} \sum_{\mathbf{k}} e^{i\mathbf{k}\cdot\mathbf{r}} S^+(\mathbf{k}), \tag{2.20}$$

$$S^+(\mathbf{k}) = \frac{1}{\sqrt{N}} \sum_{i} e^{-i\mathbf{k}\cdot\mathbf{r}} S_i^+, \tag{2.21}$$

and for the spin lowering operators $S_i^- \equiv S_i^x - iS_i^y$:

$$S_i^- = \frac{1}{\sqrt{N}} \sum_{\mathbf{k}} e^{i\mathbf{k}\cdot\mathbf{r}} S^-(\mathbf{k}), \tag{2.22}$$

$$S^-(\mathbf{k}) = \frac{1}{\sqrt{N}} \sum_{i} e^{-i\mathbf{k}\cdot\mathbf{r}} S_i^-. \tag{2.23}$$

Note that according to these definitions we have $\mathbf{S}(-\mathbf{k}) = [\mathbf{S}(\mathbf{k})]^\dagger$ and $S^-(-\mathbf{k}) = [S^+(\mathbf{k})]^\dagger$.

Let's now reexpress the Hamiltonian (2.14) in terms of the Fourier transformed operators. For the exchange and Zeeman terms, the transformation is straightforward:

$$H_{ex} = -J \sum_{\mathbf{k}} \sum_{\boldsymbol{\delta}} e^{i\mathbf{k}\cdot\boldsymbol{\delta}} \left[S^x(\mathbf{k}) S^x(-\mathbf{k}) + S^y(\mathbf{k}) S^y(-\mathbf{k}) + S^z(\mathbf{k}) S^z(-\mathbf{k}) \right], \tag{2.24}$$

where $\boldsymbol{\delta}$ is a vector from a site to any of its nearest neighbor site, and

$$H_Z = -g\mu_B H_0 \sqrt{N} S^z(\mathbf{k} = 0). \tag{2.25}$$

For the dipolar interaction, the transformation to wavevector space is more complicated due to its long-ranged nature. We first note that the dipolar interaction (2.17) could be written in a simpler form:

$$H_d = \frac{1}{2} \left(g\mu_B \right)^2 \sum_{i \neq j} S_i^\alpha S_j^\beta \partial_{\alpha_i} \partial_{\beta_j} \frac{1}{r_{ij}}, \tag{2.26}$$

where α and β are summed over x, y, z. In getting this expression we used $\partial_{\alpha_i} \partial_{\beta_j} (1/r_{ij}) = \delta^{\alpha\beta}/r_{ij}^3 - 3 r_{ij}^\alpha r_{ij}^\beta / r_{ij}^5$. Next we make use of the film geometry where the thickness (in the y-direction) is much less than the other two dimensions. We will adopt the so-called " uniform mode approximation" [13], which assumes the magnetization in y-direction to be a constant, and replaces it by its average value over y-coordinate. This means that in the expression of H_d we will make the following replacement:

$$S^\alpha(x_i, y_i, z_i) \to \int \frac{dy_i'}{d} S^\alpha(x_i, y_i', z_i), \tag{2.27}$$

$$S^\beta(x_j, y_j, z_j) \to \int \frac{dy_j'}{d} S^\beta(x_j, y_j', z_j). \tag{2.28}$$

We will also temporarily view the lattice as a continuous media, so the summations $\sum_{i \neq j}$ are

replaced by integrals:

$$\sum_{i\neq j} \to \int \frac{N^2 dx_i dy_i dz_i dx_j dy_j dz_j}{V^2} \equiv \int \frac{N^2 d\mathbf{r}_i d\mathbf{r}_j}{V^2}. \tag{2.29}$$

The dipolar interaction then reads:

$$H_d = \frac{1}{2}\left(g\mu_B\right)^2 \int \frac{N^2 d\mathbf{r}_i d\mathbf{r}_j}{V^2} \left(\int \frac{dy_i'}{d} S^\alpha(x_i, y_i', z_i)\right) \left(\int \frac{dy_j'}{d} S^\beta(x_j, y_j', z_j)\right) \partial_{\alpha_i}\partial_{\beta_j} \frac{1}{r_{ij}}, \tag{2.30}$$

where $V = Ad$ is the volume of the material. Next make use of the expression

$$\frac{1}{r_{ij}} = \frac{4\pi}{A} \sum_{\mathbf{k}_\parallel} e^{i\mathbf{k}_\parallel \cdot \mathbf{r}_{\parallel,ij}} G_{k_\parallel}\left(y_i - y_j\right), \tag{2.31}$$

$$G_{k_\parallel}(y) = \frac{e^{-k_\parallel |y|}}{2k_\parallel}, \tag{2.32}$$

where $\mathbf{k}_\parallel = k_x\hat{x} + k_z\hat{z}$ is a wavevector in the xOz plane, $\mathbf{r}_{\parallel,ij} = (x_i - x_j)\hat{x} + (z_i - z_j)\hat{z}$ is the xOz-plane projection of $\mathbf{r}_{ij}$, and $G_{k_\parallel}(y)$ is the Green function of an 1D Helmholtz equation:

$$\left(d_y^2 - k_\parallel^2\right) G_{k_\parallel}\left(y\right) = -\delta\left(y\right). \tag{2.33}$$

Putting (2.31) into (2.30), we get:

$$\begin{aligned} H_d = {} & \frac{1}{2}\left(g\mu_B\right)^2 \int \frac{N^2 d\mathbf{r}_i d\mathbf{r}_j}{V^2} \left(\int \frac{dy_i'}{d} S^\alpha(x_i, y_i', z_i)\right) \left(\int \frac{dy_j'}{d} S^\beta(x_j, y_j', z_j)\right) \\ & \times \partial_{\alpha_i}\partial_{\beta_j} \frac{4\pi}{A} \sum_{\mathbf{k}_\parallel} e^{i\mathbf{k}_\parallel \cdot \mathbf{r}_{\parallel,ij}} G_{k_\parallel}\left(y_i - y_j\right). \end{aligned} \tag{2.34}$$

Recall that α and β are summed over x, y, z. Let's consider the possible cases of these summations. When both α and β are x or z, the two derivatives $\partial_{\alpha_i}\partial_{\beta_j}$ generate $k_\parallel^\alpha k_\parallel^\beta$. When only one of the two indices is y, say $\alpha = y$, then ∂_{α_i} acts on $G_{k_\parallel}\left(y_i - y_j\right)$. But the integral $\int dy_i \int dy_j \partial_{y_i} G_{k_\parallel}\left(y_i - y_j\right)$ would vanish, since $G_{k_\parallel}\left(y_i - y_j\right)$ is an even function of $y_i - y_j$. So the case that only one of the two indices is y would give no contribution to H_d. Finally, when both α and β are y, we would get

the integral $\int dy_i \int dy_j \partial_{y_i}\partial_{y_j} G_{k_\parallel}(y_i - y_j)$. Therefore,

$$
\begin{aligned}
H_d &= \frac{1}{2}(g\mu_B)^2 \int \frac{N^2 d\mathbf{r}_i d\mathbf{r}_j}{V^2} \left(\int \frac{dy_i'}{d} S^\alpha(x_i, y_i', z_i)\right)\left(\int \frac{dy_j'}{d} S^\beta(x_j, y_j', z_j)\right) \\
&\times \frac{4\pi}{A}\sum_{\mathbf{k}_\parallel} k_\parallel^\alpha k_\parallel^\beta e^{i\mathbf{k}_\parallel\cdot\mathbf{r}_{\parallel,ij}} G_{k_\parallel}(y_i - y_j) \\
&+ \frac{1}{2}(g\mu_B)^2 \int \frac{N^2 d\mathbf{r}_i d\mathbf{r}_j}{V^2} \left(\int \frac{dy_i'}{d} S^y(x_i, y_i', z_i)\right)\left(\int \frac{dy_j'}{d} S^y(x_j, y_j', z_j)\right) \\
&\times \frac{4\pi}{A}\sum_{\mathbf{k}_\parallel} e^{i\mathbf{k}_\parallel\cdot\mathbf{r}_{\parallel,ij}} \partial_{y_i}\partial_{y_j} G_{k_\parallel}(y_i - y_j)\,. \qquad (2.35)
\end{aligned}
$$

Now we rewrite the integral $\int dx_i dz_i dx_j dz_j dy_i' dy_j'$ back to the discrete form, and use the expression of Fourier transformation of $\mathbf{S}$ (Eq. (2.19)):

$$
\begin{aligned}
H_d &= \frac{1}{2}(g\mu_B)^2 \frac{4\pi N}{A}\sum_{\mathbf{k}_\parallel} S^\alpha(-\mathbf{k}_\parallel) S^\beta(\mathbf{k}_\parallel) k_\parallel^\alpha k_\parallel^\beta \int \frac{dy_i dy_j}{d^2} G_{k_\parallel}(y_i - y_j) \\
&+ \frac{1}{2}(g\mu_B)^2 \frac{4\pi N}{A}\sum_{\mathbf{k}_\parallel} S^y(-\mathbf{k}_\parallel) S^y(\mathbf{k}_\parallel) \int \frac{dy_i dy_j}{d^2} \partial_{y_i}\partial_{y_j} G_{k_\parallel}(y_i - y_j)\,. \qquad (2.36)
\end{aligned}
$$

Performing the integrals over y_i and y_j, we get the expression of dipolar interaction in wavevector space:

$$
H_d = \frac{2\pi N}{V}(g\mu_B)^2 \sum_{\mathbf{k}_\parallel}\left[(1 - F_{k_\parallel})\frac{k_\parallel^\alpha k_\parallel^\beta}{k_\parallel^2} S^\alpha(-\mathbf{k}_\parallel) S^\beta(\mathbf{k}_\parallel) + F_{k_\parallel} S^y(-\mathbf{k}_\parallel) S^y(\mathbf{k}_\parallel)\right], \qquad (2.37)
$$

where we defined the "form factor"

$$
F_k = \frac{1 - e^{-kd}}{kd}. \qquad (2.38)
$$

Note that although in the first term in (2.37) the indices α and β are formally summed over x, y, z, only the terms with $\alpha, \beta = x, z$ will be nonzero, since $\mathbf{k}_\parallel = k_x\hat{x} + k_z\hat{z}$ has no y-components.

Writing out those terms separately, we get:

$$H_d = \frac{2\pi N}{V}(g\mu_B)^2 \sum_{\mathbf{k}_\parallel} \Big\{ (1 - F_{k_\parallel}) \left[\sin^2\theta S^x(-\mathbf{k}_\parallel) S^x(\mathbf{k}_\parallel) + \cos^2\theta S^z(-\mathbf{k}_\parallel) S^z(\mathbf{k}_\parallel) \right.$$
$$\left. + \sin\theta\cos\theta S^x(-\mathbf{k}_\parallel) S^z(\mathbf{k}_\parallel) + \sin\theta\cos\theta S^z(-\mathbf{k}_\parallel) S^x(\mathbf{k}_\parallel) \right] + F_{k_\parallel} S^y(-\mathbf{k}_\parallel) S^y(\mathbf{k}_\parallel) \Big\}, \quad (2.39)$$

where we introduced the angle between $\mathbf{k}_\parallel$ and the z-axis as θ, so that $k_x = k_\parallel \sin\theta$, $k_z = k_\parallel \cos\theta$.

Note that in this expression of H_d in wavevector space, summation over only 2D wavevectors in the xOz plane are involved, which is due to the uniform mode approximation we used. Thus, although in the previous expression of exchange Hamiltonian (2.24) the summation is over 3D wavevectors, later we will consider wavevectors only in the xOz plane. In summary, we get the following Hamiltonian in 2D wavevector space:

$$H = H_{ex} + H_Z + H_d$$
$$= -J \sum_{\mathbf{k}_\parallel} \sum_{\boldsymbol{\delta}} e^{i\mathbf{k}_\parallel \cdot \boldsymbol{\delta}} \left[S^x(\mathbf{k}_\parallel) S^x(-\mathbf{k}_\parallel) + S^y(\mathbf{k}_\parallel) S^y(-\mathbf{k}_\parallel) + S^z(\mathbf{k}_\parallel) S^z(-\mathbf{k}_\parallel) \right] - g\mu_B H_0 \sqrt{N} S^z(\mathbf{k}=0)$$
$$+ \frac{2\pi N}{V}(g\mu_B)^2 \sum_{\mathbf{k}_\parallel} \Big\{ (1 - F_{k_\parallel}) \left[\sin^2\theta S^x(-\mathbf{k}_\parallel) S^x(\mathbf{k}_\parallel) + \cos^2\theta S^z(-\mathbf{k}_\parallel) S^z(\mathbf{k}_\parallel) \right.$$
$$\left. + \sin\theta\cos\theta S^x(-\mathbf{k}_\parallel) S^z(\mathbf{k}_\parallel) + \sin\theta\cos\theta S^z(-\mathbf{k}_\parallel) S^x(\mathbf{k}_\parallel) \right] + F_{k_\parallel} S^y(-\mathbf{k}_\parallel) S^y(\mathbf{k}_\parallel) \Big\}. \quad (2.40)$$

For simplicity, from now on we will write $\mathbf{k}$ instead of $\mathbf{k}_\parallel$, while keeping in mind that $\mathbf{k}$ is a 2D vector in the xOz plane.

2.3.2 Holstein-Primakoff transformation

As stated before, magnons are bosonic excitations from a ferromagnetic ground state. But our current Hamiltonian is in terms of spin operators instead of bosonic operators. The change from spin system to a bosonic system is accomplished via the Holstein-Primakoff transformation [9],

which we describe in this subsection. This transformation is written as:

$$S_i^+ = \sqrt{2S - a_i^\dagger a_i} a_i, \tag{2.41}$$

$$S_i^- = a_j^\dagger \sqrt{2S - a_i^\dagger a_i}, \tag{2.42}$$

$$S_i^z = S - a_i^\dagger a_i, \tag{2.43}$$

where a_i ($a_j^\dagger$) is a bosonic annihilation (creation) operator for the site i, which satisfies standard bosonic commutation relations:

$$[a_i, a_j] = [a_i^\dagger, a_j^\dagger] = 0, \tag{2.44}$$

$$[a_i, a_j^\dagger] = \delta_{ij}. \tag{2.45}$$

One can check that the commutation relations for the spin operators (2.1) are recovered by plugging in directly the transformation (2.41)-(2.43) and using (2.44) and (2.45). This means that the Holstein-Primamoff transformation is an exact mapping from spin operators to bosonic operators.

Let's look at the physical meaning of the bosonic operators. According to Eqs. (2.41)-(2.42), $a^\dagger$ acting on any state increases the projection by 1, where $a^\dagger$ acting on any state decreases the projection by 1. In the case that the state with maximal projection ($|S, m_s = +S\rangle$) is the ground state (which will be the situation in our later considerations), then $a^\dagger$ creates to an excitation from this ground state. Besides, (2.42) says that the number of bosons for a given state ($a^\dagger a$) is equal to the difference of the maximal projection (S) and the projection of that state.

After performing the Holstein-Primakoff transformation, a Hamiltonian in terms of spin operators is transferred to one in terms of bosonic operators. Generally a bosonic Hamiltonian is more easily to handle as compared to a spin Hamiltonian. Thus, the Holstein-Primakoff transformation is expected to be very useful. However, there is a technical difficulty for its applications: the appearance of operators under square roots. To overcome this, approximations

are usually needed. In (2.41) and (2.42), let's expand the square roots in orders of $1/S$:

$$S_i^+ = \sqrt{2S}[a_i - \frac{1}{4S}a_i^\dagger(a_i)^2 + O(\frac{1}{S^2})], \tag{2.46}$$

$$S_i^- = \sqrt{2S}[a_i^\dagger - \frac{1}{4S}(a_i^\dagger)^2 a_i + O(\frac{1}{S^2})]. \tag{2.47}$$

If we focus on the configurations close to the ground state, namely, if the states we are considering have number of bosons for any site i satisfying $\langle a_i^\dagger a_i\rangle \ll S$, then it will be a good approximation to keep the leading order terms in the expansions (2.46) and (2.47).

2.3.3 Hamiltonian in terms of bosonic operators

Let's now employ the Holstein-Primakoff transformation in our treatment of the magnetic system described by the Hamiltonian (2.14), and by (2.40) in the wavevector space. Like for the spin operators, we define Fourier transformation of the bosonic operators:

$$a_i = \frac{1}{\sqrt{N}}\sum_{\mathbf{k}} e^{i\mathbf{k}\cdot\mathbf{r}}a_{\mathbf{k}}, \tag{2.48}$$

$$a_{\mathbf{k}} = \frac{1}{\sqrt{N}}\sum_{i} e^{-i\mathbf{k}\cdot\mathbf{r}}a_i. \tag{2.49}$$

In terms of $a_{\mathbf{k}}$ and $a_{\mathbf{k}}^\dagger$, Fourier transformation of the spin operators reads:

$$S^+(\mathbf{k}) = \sqrt{2S}\left(a_{\mathbf{k}} - \frac{1}{4SN}\sum_{\mathbf{q},\mathbf{q}'} a^\dagger_{\mathbf{q}+\mathbf{q}'-\mathbf{k}}a_{\mathbf{q}}a_{\mathbf{q}'} + O(\frac{1}{S^2})\right), \tag{2.50}$$

$$S^-(-\mathbf{k}) = \sqrt{2S}\left(a^\dagger_{\mathbf{k}} - \frac{1}{4SN}\sum_{\mathbf{q},\mathbf{q}'} a^\dagger_{\mathbf{q}}a^\dagger_{\mathbf{q}'}a_{\mathbf{q}+\mathbf{q}'-\mathbf{k}} + O(\frac{1}{S^2})\right), \tag{2.51}$$

$$S^z(\mathbf{k}) = \sqrt{N}S\delta_{\mathbf{k},0} - \frac{1}{\sqrt{N}}\sum_{\mathbf{q}} a^\dagger_{\mathbf{q}}a_{\mathbf{q}+\mathbf{k}}. \tag{2.52}$$

Putting these expressions into (2.40) and using $S^\pm(\mathbf{k}) = S^x(\mathbf{k}) \pm iS^y(\mathbf{k})$, we could obtain a Hamiltonian expressed by bosonic operators $a_{\mathbf{k}}$ and $a_{\mathbf{k}}^\dagger$.

2.3.3.1 Without dipolar interaction

Let's first consider the case when there is no dipolar interaction. The Hamiltonian in wavevector space reads:

$$\begin{aligned} H &= H_{ex} + H_Z \\ &= -J \sum_{\mathbf{k}} \sum_{\boldsymbol{\delta}} e^{i\mathbf{k}\cdot\boldsymbol{\delta}} \left[S^x(\mathbf{k}) S^x(-\mathbf{k}) + S^y(\mathbf{k}) S^y(-\mathbf{k}) + S^z(\mathbf{k}) S^z(-\mathbf{k}) \right] - g\mu_B H_0 \sqrt{N} S^z(\mathbf{k}=0) \\ &= -\frac{J}{2} \sum_{\mathbf{k}} \sum_{\boldsymbol{\delta}} e^{i\mathbf{k}\cdot\boldsymbol{\delta}} \left[S^+(\mathbf{k}) S^-(-\mathbf{k}) + S^-(\mathbf{k}) S^+(-\mathbf{k}) + 2S^z(\mathbf{k}) S^z(-\mathbf{k}) \right] - g\mu_B H_0 \sqrt{N} S^z(\mathbf{k}=0). \end{aligned} \tag{2.53}$$

Note that here $\mathbf{k}$ can be understood as a 3D wavevector. Plugging Eqs. (2.50), (2.51) and (2.52) into this Hamiltonian and keeping terms up to second order in $a_{\mathbf{k}}$ and $a_{\mathbf{k}}^\dagger$, we get:

$$H = -6JS^2 N - g\mu_B H_0 SN + \sum_{\mathbf{k}} \left[g\mu_B H_0 + 2JS \sum_{\boldsymbol{\delta}} (1 - e^{i\mathbf{k}\cdot\boldsymbol{\delta}}) \right] a_{\mathbf{k}}^\dagger a_{\mathbf{k}}. \tag{2.54}$$

Let's examine the different terms of this Hamiltonian. The constant terms correspond to the ground state energy. (The coefficient 6 is the number of nearest neighbors for a site in a simple cubic lattice.) It can also be obtained directly by acting the original spin Hamiltonian on the ground state in which $|S, m_s = +S\rangle$ for every site.

The quadratic term corresponds to energy of excitations from the ground state. We note that only terms of the form $a_{\mathbf{k}}^\dagger a_{\mathbf{k}}$ appear, so the number of excitations corresponding to the $a_{\mathbf{k}}$ and $a_{\mathbf{k}}^\dagger$ operators is conserved. We can then recognize the $a_{\mathbf{k}}$ and $a_{\mathbf{k}}^\dagger$ operators as annihilation and creation operators of a magnon, which has well-defined momentum and energy. In particular, $a_{\mathbf{k}}^\dagger$ creates a magnon with wavevector $\mathbf{k}$ and energy $g\mu_B H_0 + 2JS \sum_{\boldsymbol{\delta}} (1 - e^{i\mathbf{k}\cdot\boldsymbol{\delta}})$. Thus, the spectrum of magnons is

$$\omega(\mathbf{k}) = g\mu_B H_0 + 2JS \sum_{\boldsymbol{\delta}} (1 - e^{i\mathbf{k}\cdot\boldsymbol{\delta}}). \tag{2.55}$$

For a simple cubic lattice, performing the summation over $\boldsymbol{\delta}$ we get:

$$\omega(\mathbf{k}) = g\mu_B H_0 + 2JS[6 - 2\cos(k_x a) - 2\cos(k_y a) - 2\cos(k_z a)]. \tag{2.56}$$

In the case that only small enough wavevectors are considered so that $k \ll 1/a$, we can expand the cosine functions and obtain the following approximate form of magnon spectrum:

$$\omega(\mathbf{k}) = g\mu_B H_0 + \mathcal{D}k^2, \tag{2.57}$$

where we introduced the exchange coupling $\mathcal{D} = 2JSa^2$. Note that in this form the spectrum is isotropic. It has a gap proportional to the external field H_0, and is quadratic in wavevector k. If there is no external field (namely only exchange interaction is considered), the magnon spectrum will be gapless with $\omega(\mathbf{k} = 0) = 0$. This means that an excitation with infinitely long wavelengths will have infinitely small energy. According to Goldstone's theorem, this gapless spectrum is a direct consequence of spontaneously breaking of the previously discussed 3D rotational symmetry of the exchange Hamiltonian.

2.3.3.2 With dipolar interaction

Now we include the dipolar interaction. In terms of $S^{\pm}(\mathbf{k})$ operators, we have

$$\begin{aligned} H_d = \frac{2\pi N}{V}(g\mu_B)^2 \sum_{\mathbf{k}} \Bigg\{ & \frac{1}{4}\left[(1-F_k)\sin^2\theta - F_k\right]\left[S^+(-\mathbf{k})S^+(\mathbf{k}) + S^-(-\mathbf{k})S^-(\mathbf{k})\right] \\ & + \frac{1}{4}\left[(1-F_k)\sin^2\theta + F_k\right]\left[S^+(-\mathbf{k})S^-(\mathbf{k}) + S^-(-\mathbf{k})S^+(\mathbf{k})\right] + (1-F_{k_\parallel})\cos^2\theta S^z(-\mathbf{k})S^z(\mathbf{k}) \\ & + \frac{1}{2}(1-F_k)\sin\theta\cos\theta\left[S^+(-\mathbf{k})S^z(\mathbf{k}) + S^z(-\mathbf{k})S^+(\mathbf{k}) + S^z(-\mathbf{k})S^-(\mathbf{k}) + S^-(-\mathbf{k})S^z(\mathbf{k})\right]\Bigg\}. \end{aligned} \tag{2.58}$$

where $\mathbf{k}$ is now understood as a 2D wavevector in the xOz plane. Plugging Eqs. (2.50), (2.51) and (2.52) into this Hamiltonian and keeping terms up to second order in $a_{\mathbf{k}}$ and $a_{\mathbf{k}}^{\dagger}$, we get:

$$H_d = \frac{\pi N}{V}\left(g\mu_B\right)^2 S \sum_{\mathbf{k}} \left[(1-F_k)\sin^2\theta + F_k\right] \\ + \frac{2\pi N}{V}\left(g\mu_B\right)^2 S \sum_{\mathbf{k}} \left\{ \left[(1-F_k)\sin^2\theta - F_k\right] a_{\mathbf{k}}^{\dagger} a_{\mathbf{k}} + \frac{1}{2}\left[(1-F_k)\sin^2\theta - F_k\right]\left(a_{\mathbf{k}} a_{-\mathbf{k}} + a_{\mathbf{k}}^{\dagger} a_{-\mathbf{k}}^{\dagger}\right)\right\}. \tag{2.59}$$

We see that, for the quadratic terms, not only terms of the form $a_{\mathbf{k}}^{\dagger} a_{\mathbf{k}}$ appear, terms of $a_{\mathbf{k}} a_{-\mathbf{k}}$ and $a_{\mathbf{k}}^{\dagger} a_{-\mathbf{k}}^{\dagger}$ appear as well. This means that the number of bosons corresponding to the $a_{\mathbf{k}}$ and $a_{\mathbf{k}}^{\dagger}$ operators is not conserved any more. Thus, inclusion of the dipolar interaction leads to a dramatic difference.

Let's now write the quadratic part of the Hamiltonian for all interactions together:

$$H^{(2)} = \sum_{\mathbf{k}} \left[\mathcal{A}_{\mathbf{k}} a_{\mathbf{k}}^{\dagger} a_{\mathbf{k}} + \frac{1}{2}\mathcal{B}_{\mathbf{k}}\left(a_{\mathbf{k}} a_{-\mathbf{k}} + a_{\mathbf{k}}^{\dagger} a_{-\mathbf{k}}^{\dagger}\right)\right], \tag{2.60}$$

where the coefficients are

$$\mathcal{A}_{\mathbf{k}} = \gamma H_0 + \mathcal{D}k^2 + \gamma 2\pi M\left[(1-F_k)\sin^2\theta + F_k\right], \tag{2.61}$$

$$\mathcal{B}_{\mathbf{k}} = \gamma 2\pi M\left[(1-F_k)\sin^2\theta - F_k\right], \tag{2.62}$$

and we have introduced the gyromagnetic ratio $\gamma = g\mu_B$ and the magnetization $M = g\mu_B NS/V$, so that $(g\mu_B)^2 NS/V = \gamma M$. Note that we have adopted the approximation of small wavevectors; in this case the exchange interaction gives a quadratic term $\mathcal{D}k^2$.

Since now the Hamiltonian (2.60) involves number-non-conserving terms, we cannot read out the spectrum directly. The standard procedure to treat a Hamiltonian like (2.60) is to perform a Bogoliubov transformation [14], which purpose is to cast the Hamiltonian into a form without the

number-non-conserving terms. Let's introduce new bosonic operators $c_{\mathbf{k}}$ and $c_{\mathbf{k}}^\dagger$ as:

$$a_{\mathbf{k}} = u_{\mathbf{k}} c_{\mathbf{k}} + v_{\mathbf{k}} c_{-\mathbf{k}}^\dagger, \tag{2.63}$$

$$a_{\mathbf{k}}^\dagger = u_{\mathbf{k}} c_{\mathbf{k}}^\dagger + v_{\mathbf{k}} c_{-\mathbf{k}}, \tag{2.64}$$

$$u_{\mathbf{k}} = \sqrt{\frac{\mathcal{A}_{\mathbf{k}} + \omega_{\mathbf{k}}}{2\omega_{\mathbf{k}}}}, \tag{2.65}$$

$$v_{\mathbf{k}} = \mathrm{sgn}(\mathcal{B}_{\mathbf{k}}) \sqrt{\frac{\mathcal{A}_{\mathbf{k}} - \omega_{\mathbf{k}}}{2\omega_{\mathbf{k}}}}, \tag{2.66}$$

$$\omega_{\mathbf{k}} = \sqrt{\mathcal{A}_{\mathbf{k}}^2 - \mathcal{B}_{\mathbf{k}}^2}. \tag{2.67}$$

The choice of coefficients $u_{\mathbf{k}}$ and $v_{\mathbf{k}}$ ensures that the operators $c_{\mathbf{k}}$ and $c_{\mathbf{k}}^\dagger$ satisfy the standard bosonic commutating relations, and that the Hamiltonian $H^(2)$ is "diagonalized", in the sense that only number-conserving terms appear:

$$H^{(2)} = \sum_{\mathbf{k}} \omega_{\mathbf{k}} c_{\mathbf{k}}^\dagger c_{\mathbf{k}}. \tag{2.68}$$

We see that, with existence of the dipolar interaction, the number-conserving excitations are not corresponding to the originally introduced operators $a_{\mathbf{k}}$ and $a_{\mathbf{k}}^\dagger$, but to the "tilted" operators $c_{\mathbf{k}}$ and $c_{\mathbf{k}}^\dagger$. These new operators now serve as the magnon operators. The quantity $\omega_{\mathbf{k}}$ is the spectrum of magnons:

$$\omega_{\mathbf{k}} = \sqrt{\mathcal{A}_{\mathbf{k}}^2 - \mathcal{B}_{\mathbf{k}}^2} = \sqrt{\left[\gamma H_0 + \mathcal{D}k^2 + \gamma 4\pi M(1 - F_k)\sin^2\theta\right](\gamma H + \mathcal{D}k^2 + \gamma 4\pi M F_k)}. \tag{2.69}$$

Let's look at this spectrum in more detail. First, if there is no dipolar interaction (namely, if we set $M = 0$), this spectrum reduces to the previous expression (2.57), as expected. Second, recalling that $F_k = (1 - e^{-kd}/(kd)$, we see that the value of F_k is always between 0 and 1. Then for a fixed k, a larger $\sin^2\theta$ will give a larger $\omega_{\mathbf{k}}$. Thus, minima of spectrum can only exist at $\theta = 0$, or when $\mathbf{k}$ is along z-direction. This means that magnons with lowest energy have wavevectors along or

opposite to the external magnetic field. The spectrum along this direction reads:

$$\omega_{\mathbf{k}} = \sqrt{(\gamma H_0 + \mathcal{D}k_z^2)\,(\gamma H_0 + \mathcal{D}k_z^2 + \gamma 4\pi M F_k)}. \tag{2.70}$$

Fig. 2.3 plots this spectrum along the z-direction (the blue curve). It is symmetric about $k_z = 0$, as expected. For comparison, the red and dashed curve shows the spectrum without the dipolar interaction (Eq. (2.57)), which is simply a parabola. We see that at large enough k_z the two curves approach each other, but at small k_z they are quite different. The dipolar interaction introduces a cusp at $k_z = 0$ and, together with the exchange interaction, produces two symmetric minima at $k_z \neq 0$. The positions of the two minima are at approximately $k_z = \pm 7.5$ μm for the parameters chosen in the figure. The fact that the dipolar interaction has a large effect at small wavevectors is consistent with its long-ranged nature. For more detailed discussions on the spectrum please see Ref. [15].

2.4 Discussions

In summary, in this chapter we considered magnons in ferromagnetic films. Starting from a Hamiltonian in terms of spin operators, we performed the Holstein-Primakoff transformation to write the Hamiltonian in terms of bosonic operators. Then after a Bogoliubov transformation (in the case when dipolar interaction is taken into account) we arrive at a Hamiltonian in terms of magnon operators, from which we obtain the spectrum of magnons. Below are discussions on several relevant points:

1. In our consideration we included only terms up to quadratic order in magnon operators. Thus, the magnons appear to be not interacting with others. Inclusion of higher order terms will generate interaction between magnons. In particular, in later chapters we will consider fourth order interaction of magnons. It will turn out to play important roles in determining properties of magnon BEC and superfluidity.

2. When treating the dipolar interaction we made the uniform mode approximation [13], which assumes that there is no modulation of magnetization in the direction transverse to the

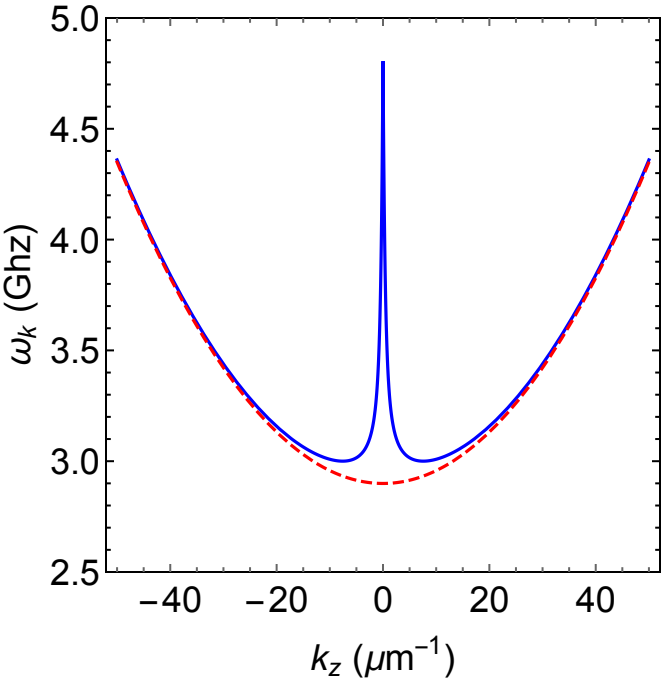

Figure 2.3: Spectrum of the magnons along the direction of the external field (z-direction). The blue and solid curve is the spectrum calculated from Eq. (2.70). The spectrum is symmetric and has two minima at $k_z = \pm 7.5$ μm. For comparison, the red and dashed curve shows the spectrum without dipolar interaction calculated from Eq. (2.57). The parameters are chosen as: $\gamma = 1.2 \times 10^{-5}$ eV/kOe, $\mathcal{D} = 0.24$ eVÅ^2, $H_0 = 1$ kOe, $4\pi M = 1.78$ kOe, and $d = 5$ μm.

film plane (the y-direction in our case). Under this approximation only the lowest band in the transverse direction is taken into account and this lowest band is taken to have zero k_y, so the system becomes effectively 2D. An improved treatment would take into account the transverse variation of magnetization, in which case the wavevectors could have non-zero components in the y-direction, and the spectrum has infinitely number of bands labelled by k_y. In the literature, since the seminal work by Damon and Eshbach [2], magnon spectrum in ferromagnetic films with transverse modulation of magnetization have been theoretically studied extensively [16, 17, 18, 19, 20, 21, 22, 23, 24]. In this work we will confine ourselves to the uniform mode approximation, thus avoiding the complications arisen from considering transverse modulation of magnetization.

3. The theory of magnons described in this chapter is of quantum-mechanical nature, namely,

it is based on spin operators. Alternatively, spin waves can also be treated purely classically by the Landau-Lifshitz equation [25, 26]. This classical treatment is generally valid when the wavelength of spin waves is much larger than the lattice constant (or equivalently when the wavevector is small), so that properties of spin waves does not depend on the microscopic details of the discrete lattice. By linearizing the Landau-Lifshitz equation the spectrum with exchange and Zeeman interactions could be derived, which will be the same as Eq. (2.57).

3. BOSE-EINSTEIN CONDENSATION OF MAGNONS IN FERROMAGNETIC FILMS*

For a long time after Einstein's prediction of the condensation for the ideal Bose-gas the only experimentally demonstrated example of this phenomenon was the transition of liquid ^{4}He to the superfluid state discovered in 1938 by Kapitza [27] and Allen and Misener [28]. They found that viscosity of ^{4}He vanishes at temperature 2.17 K and normal pressure. F. London was the first to propose that this phenomenon is associated with the Bose-Einstein condensation (BEC) [29]. L.D. Landau [30] found a criterion to the excitation spectrum of a quantum Bose-liquid, that must be satisfied in order for the liquid to become superfluid at low enough temperature. N.N. Bogoliubov [14] extended the idea of BEC to the weakly interacting Bose-gas and found its spectrum that indeed satisfied the Landau criterion.

It took nearly 70 years before Wieman, Cornell and Ketterle discovered two other systems displaying BEC, both of them being laser-cooled gases of alkali atoms (potassium and sodium) [31, 32]. They condensed at temperatures of a few hundreds nanokelvin. Later experiments identified the quantized vortex lines in these gases driven by rotation of the gas as a whole [33]. This discovery was considered a definitive proof of superfluidity.

The beginning of this century brought new systems where BEC were observed. They were gases of excitations (quasiparticles) rather than atomic gases or liquids, specifically: i) magnons in a ferrite film [1]; ii) excitons-polaritons in quantum dots [34]; iii) photons in a microcavity filled by a gas of dye molecules [35]. In the cases i) and iii) Bose-condensation proceeded at room temperature. Zero-dimensional geometry of the condensation of photons and excitons-polaritons disallowed the study of transport properties. The magnon condensation was instead studied in a macroscopic film. It thus provides a good platform for studying transport properties related to BEC.

*Part of this chapter uses material with permission from "Bose-Einstein condensation and superfluidity of magnons in yttrium iron garnet films" by Chen Sun, Thomas Nattermann and Valery L. Pokrovsky, 2017, Journal of Physics D: Applied Physics, 2017, 50, 143002, Published 7 March 2017, DOI: https://doi.org/10.1088/1361-6463/aa5cfc, Copyright 2017 by IOP Publishing

In this chapter, we discuss BEC of magnons in ferromagnetic films. We will start with discussing magnetic properties of the material yttrium iron garnet (YIG) on which magnon BEC was discovered. We then talk about the experimental facts of BEC of magnons, and the theory describing it. We also discuss an alternative classical interpretation of the magnon condensate. In the next chapter when we consider superfluidity of magnons, the knowledge of magnon BEC will be useful.

3.1 Yttrium iron garnet

Yttrium iron garnet (YIG) [36] is a synthetic garnet with chemical composition $Y_3Fe_5O_{12}$. Its crystalline structure is body-center cubic, with a lattice constant $a = 1.24$ nm. The structure is quite complex – there are 80 atoms in each elementary cell. 20 of them are Fe^{3+} ions, which occupies 8 octahedral and 12 tetrahedral sites. Couplings between these iron ions from different kinds of sites are antiferromagnetic, and ions in the two kinds of sites exhibit different spins. These result in partial compensation of spins in an elementary cell, which determines YIG to be ferrimagnetic. The average spin per elementary cell is $S = 14.5$ at room temperature.

YIG has a very high Curie temperature $T_c = 560$ K. Thus, at room temperature it is well inside the ferromagnetic phase. Magnons in YIG has very small attenuation with a Gilbert damping as low as $\alpha \sim 10^{-4}$. Estimate from magnon-phonon interaction gives a characteristic attenuation time $\sim 1\ \mu$s. YIG has been used in microwave, acoustic, optical, and magneto-optical devices, e.g. in microwave YIG filters.

With 20 magnetic ions in a unit cell, the spectrum of magnons in YIG is very complicated [36]. But if we are only interested in low-energy excitations, we could ignore the distribution of spins on iron ions inside a unit cell and treat each cell to have a single total spin S. Adopting this approximation, the material can be effectively viewed as ferromagnetic, and the model described in the previous chapter can be used to describe magnons in YIG.

3.2 Experimental discovery of Bose-Einstein condensation of magnons

3.2.1 Basic experimental facts

In 2006, the discovery of BEC of magnons was reported in a seminal work by S.O. Demokritov and coworkers [1]. In the experiment, they pumped the magnons using a microstrip resonator into a film of YIG at room temperature. A microwave photon from the resonator was converted into two magnons with opposite momenta and frequency ω_p equal to $1/2$ of the photon frequency. As discussed in the previous chapter, in ferromagnetic film the magnons spectrum has two symmetric minima at wave vectors $\pm\mathbf{Q}$ directed along and opposite to the external magnetic field, which is applied in the film plane. The energy gap in the magnon spectrum for thick films (2 to 6 μm in the experiment) is roughly equal to the Zeeman energy $\Delta = \gamma H_0$. The values of magnetic field and the frequency of pumped magnons were selected to satisfy the inequality $\omega_p < 2\Delta$. Then the decay processes of the pumped magnons and magnons with lower energy are forbidden by the energy conservation and only the elastic scattering of magnons is possible. At this processes the number of magnons is conserved. It does not mean that the processes violating the conservation of number of magnons are completely forbidden. The dipolar interaction enables thermal magnon to radiate a low-energy magnon via Cherenkov process and inverse process of merging of a low-energy and high-energy magnons. The energy of high-energy magnon participating in these processes must be higher than a threshold value that is much larger than Δ. At such high energy the dipolar interaction is much weaker than the exchange interaction. The ratio of velocities of these magnons is very high yielding additional kinematic suppression of these processes due to small Mach angle. Therefore, the lifetime τ_l of the low-energy magnons is much longer than their relaxation time τ_r determined by scattering processes. The number of low energy particles is conserved during the relaxation. Therefore, the pumping establishes a quasi-equilibrium distribution with non-zero chemical potential μ. In the absence of pumping the equilibrium distribution of the magnons establishes during the longer decay time (lifetime) τ_l. Thus, in the state of equilibrium the value of chemical potential is $\mu = 0$. The chemical potential of quasi-equilibrium magnon gas grows

with the pumping power W at a fixed temperature T. At a critical value of power it reaches the value Δ. As the power increases further, the chemical potential remains equal to Δ, and excessive magnons go to the condensate. In the study [1] the authors indeed observed a dramatic increase of the magnon population with minimal energy and narrowing of its line-width, much less than the corresponding value for non-coherent magnons with the same energy.

In 2012, researchers in the same group observed an interference pattern from superposition of two condensates at the two minima [3]. They identified the signal from condensate in the Brilloin light scattering (BLS) [37, 38]. Scanning the laser spot along two lateral directions of the YIG film, they have found that the intensity of the BLS signal changes periodically vs. coordinate in the direction of magnetization (or that of the magnetic field) with the wave vector $2\mathbf{Q}$. The BLS signal is proportional to the variation of magnetization in the light spot. This variation is proportional to the square of the condensate wave function:

$$\psi\left(\mathbf{x}\right)=\psi_{+}e^{i\mathbf{Q}\cdot\mathbf{x}}+\psi_{-}e^{-i\mathbf{Q}\cdot\mathbf{x}}, \tag{3.1}$$

where $\psi_{\pm}=\sqrt{N_{\pm}/V}e^{i\phi_{\pm}}$ are the condensates amplitudes at the two minima of energy, $N_{\pm}$ are the number of magnons in each condensate and $\phi_{\pm}$ are their phases, and V is the volume of the sample. In terms of the number-phase variable we find for the total condensate density:

$$n\left(\mathbf{x}\right)=n_{+}+n_{-}+2\sqrt{n_{+}n_{-}}\cos\left(2\mathbf{Q}\cdot\mathbf{x}+\phi_{+}-\phi_{-}\right). \tag{3.2}$$

Here $n_{\pm}=N_{\pm}/V$ are densities of the two condensates. In the experiment the contrast of the interference pattern $\beta=(n_{max}-n_{min})/n_{min}$ was rather low (5-10%). This can be explained by spontaneous breaking of the reflection symmetry of the two minima, which we will show by theoretical arguments later.

3.2.2 Explanation of condensation at room temperature

The fact that BEC of magnons can exist at room temperature is astonishing. To understand why, let us consider how the chemical potential is related to the total number of pumped magnons. A simple equation for this relation was first derived in the review by Bunkov and Volovik [39]. It was based on the concept discussed previously: before the pumping begun the magnons were in equilibrium with chemical potential equal to zero, whereas under pumping they acquire a finite chemical potential μ. The magnon occupation number of a state with energy ε before the pumping is $f_0(\varepsilon) = T/\varepsilon$ and becomes $f(\varepsilon) = T/(\varepsilon - \mu)$ after the relaxation. We apply the Rayleigh-Jeans distribution since only magnons with energy $\varepsilon \ll T$ are pumped. Since the occupation numbers are increased by pumping, μ is positive. Thus, the density of pumped magnons is:

$$n_p = \int_{\Delta}^{\infty} [f(\varepsilon) - f_0(\varepsilon)]\nu(\varepsilon)d\varepsilon. \tag{3.3}$$

The magnon density of state $\nu(\varepsilon)$ at large energies $\varepsilon \gg \Delta, \gamma M$ grows as $\sqrt{\varepsilon}$. Therefore, the integral in (3.3) converges. The characteristic energy of pumped magnons is of the order of μ. Eq. (3.3) determines the chemical potential μ as a function of density of pumped magnons. μ is a monotonically growing function of n_p. The chemical potential μ cannot exceed the energy gap Δ. Therefore, the density of pumped magnons defined by Eq. (3.3) does not exceed a critical value n_{pc} determined by Eq. (3.3) at $\mu = \Delta$.

On the other hand the density of pumped magnons at a stationary pumping is proportional to the absorbed pumping power W_p:

$$n_p = \frac{W_p \tau_l}{V \hbar \omega_p}. \tag{3.4}$$

Thus, the number of pumped magnons is uniquely determined by the pumping power. When W_p exceeds a critical value $W_{pc} = n_{pc} V \hbar \omega_p / \tau_l$, the difference $n_p - n_{pc}$ falls into the state with minimal energy Δ, i.e. condensate. It means that the density of the condensate is also uniquely determined

by the pumping power.

Despite the high temperature of the normal magnons, the pumped magnons, as is clear from Eq. (3.3) have very low energy of the order of Δ. Only these magnons participate in the BECM. The room temperature does not interfere with the condensation because the interaction of the low-energy with high-energy magnons is weak. It leads to non-conservation of the number of pumped magnons in the time interval τ_l, which is much much longer than the relaxation time. Condensation can only be possible if pumped magnons do not enter the high energy range. This restriction would not be satisfied if they have a temperature different from the temperature of normal magnons as it was proposed in the work [40].

While only the low-energy magnons contribute to the total number of magnons, it is not so in case of energy. A formal calculation of the contribution of pumped magnon to energy yields divergence. This shows that the pumped energy goes far to the thermal region and causes negligibly small increase of temperature $\Delta T \sim (W_p \tau_r(T))/C$, where $\tau_r(T)$ is the relaxation time of thermal magnons and C is the specific heat of the magnon system. By the order of magnitude $\tau_r(T) \sim 10^{-12}$ s at room temperature and $\Delta T \sim 10^{-2}$ K at the pumping power 1W. As we mentioned earlier the part of the pumping power W_p absorbed by the magnon gas is much less than the total power. Thus, the heating effect is even less than our estimate.

Let us compare this simplified theory with the experiment by Demidov et al. [41]. It shows that pumping of magnons into the YIG film starts when the power of the microstrip resonator W_r exceeds some threshold value W_{th}. This can be expected since the process of conversion of a photon into two magnons in the classical limit turns into the parametric resonance. It is well known that the latter process starts with a threshold power. Therefore, only part of the resonator power $W_r - W_{th}$ goes to the pairs of pumped magnons. Indeed, the experiment confirmed that the condensate density is proportional to $W_r - W_{th}$. However, only a small part of this power remains with the pumped particles, the rest goes to thermal magnons, to phonons and presumably beyond the YIG film. Indeed the estimate of the absorbed pumping power W_p using Eq. (3.4) at reasonable experimental values $n_p = 10^{18}$ cm^{-3}, $\tau = 3$ μs, half-frequency of pumping $\omega_p = 4$

GHz, the thickness of the film $d = 5$ μm and two other linear sizes $L = 1$ mm, gives $W_p = 0.001$ W, whereas the power $W_r - W_{th}$ in the experiment reached the value 0.33 W. Another experimental observation of the same work [41] is that, after condensate is formed the population of the state with $Q = 0$ (maximum of energy) saturates and stops to vary when the power W_r continues to grow. This fact is in agreement with the theory, which states that after condensation, chemical potential assumes permanent value $\mu = \Delta$. The occupation number of any non-condensate state with energy ϵ acquires a permanent value equal to $f(\varepsilon) = T/(\varepsilon - \Delta)$. The third important experimental finding of this study was that the relaxation (thermalization) time at pumping power exceeding the threshold value, decreases with $W_r - W_{th}$ growing, but after appearance of condensate it changes much slower or becomes saturated. This is also in agreement with the theory: once the density of low-energy particles increases, their collisions become more frequent. After the formation of condensate the density of normal particles remains constant.

3.3 Theory of Bose-Einstein condensation of magnons

The condensate state of non-interacting magnons in a film is degenerate in contrast with the same state in the bulk. This happens because the energy does not change redistribution of the magnons between two minima without changing their total number in condensate. This degeneration is lifted by interaction between magnons [4].

Let $\psi_\pm = \sqrt{n_\pm} e^{i\phi_\pm}$ be the amplitudes of the condensates corresponding to the two minima of magnon energy at the wave vectors $\pm\mathbf{Q}$, the same as in the previous section; $n_\pm$ and $\phi_\pm$ are the densities and phases of these two condensates. The magnon interaction is described by terms of higher power than quadratic in the expansion of the energy in powers of the condensate amplitudes and their complex conjugated values. The leading terms are cubic and of the fourth power. The energy should conform to the requirements of translational invariance and reality. The translational invariance requires the sum of momenta in each term of the expansion to be zero (the momenta of complex conjugated amplitudes must be accounted with opposite sign). Since the momenta of condensates are $\pm\mathbf{Q}$, there is no cubic terms that satisfy the condition for translational invariance. For this energy we also require that the symmetry of exchange between $+$ and $-$ is satisfied, and

that the interaction coefficients are real. The most general fourth power density of the interaction energy satisfying these conditions reads:

$$H_{int} = \frac{A}{2}\left(|\psi_+|^4 + |\psi_-|^4\right) + B|\psi_+|^2|\psi_-|^2 \\ + \frac{C}{2}\left(|\psi_+|^2 + |\psi_-|^2\right)\left(\psi_+\psi_- + \psi_+^*\psi_-^*\right) + \frac{D}{2}\left(\psi_+^2\psi_-^2 + \psi_+^{*2}\psi_-^{*2}\right). \quad (3.5)$$

Here A, B, C, D are the interaction coefficients; stars denote the complex conjugation. Fig. (3.1) presents typical diagrams for the terms appearing in this interaction energy. The physical meanings of the terms with coefficients A and B are obvious: the first is the energy of interaction between two magnons from the same condensate, the second is the energy of interaction between two magnons from different condensates. They conserve the number of magnons. On the other hand, the terms with coefficients C and D do not conserve the number of magnons. If only the exchange and Zeeman interactions are taken into account, then the Hamiltonian would only contain terms that conserve the total number of magnons. Thus, we make an important observation that the existence of C and D terms is due to the dipolar interaction only. The coefficients C and D are small in comparison with A and B at least in thick films, but these terms violate the U(1) symmetry of multiplication of the wave functions with arbitrary phase factor $e^{i\phi}$. The coefficient D was introduced in [42]. In terms of the density-phase variables the interaction energy reads:

$$H_{int} = \frac{A}{2}\left(n_+^2 + n_-^2\right) + Bn_+n_- + C\sqrt{n_+n_-}\,(n_+ + n_-)\cos\phi + Dn_+n_-\cos 2\phi, \quad (3.6)$$

where $\phi = \phi_+ + \phi_-$. Note that the energy (3.6) depends only on one phase variable ϕ and does not depend on the second variable $\bar{\phi} = \phi_+ - \phi_-$. We will discuss the physical meaning of this fact at the end of this section.

Minimization of energy (3.6) proceeds in two steps. First we minimize it over the angle ϕ at fixed densities. All constants in (3.6) must be real to ensure the real value of the condensate energy. At negative D, the minimum is reached either at $\phi = 0$ if C is also negative or at $\phi = \pi$ if C is positive. We will not consider more complicated case for positive D since calculations show that

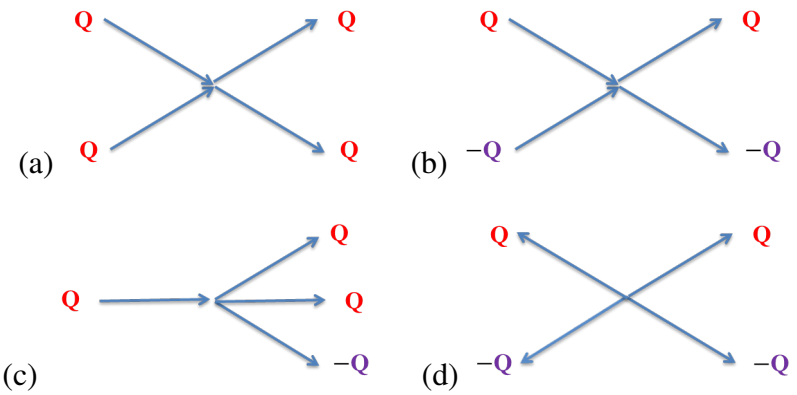

Figure 3.1: Diagram of typical process for each term in the interaction energy (3.5): (a) $A : 2 \to 2$ process for the same condensate; (b) $B : 2 \to 2$ process between different condensates; (c) $C : 1 \to 3$ or $3 \to 1$ process; (d) $D : 0 \to 4$ or $4 \to 0$ process.

D is negative for all values of the thickness and magnetic field studied thus far. Thus, the phase is trapped at one of the two values corresponding to different states of the condensate. The transition from the "0 state" to the "π state" proceeds along the curve $C = 0$ in the d-H plane. This simple calculation shows how phase trapping emerges in ferromagnetic films. It also clearly demonstrates that phase trapping is caused by magnetic dipolar interaction. The trapping of phase establishes coherence between the two condensates.

After minimization over ϕ, the interaction energy for the densities can be obtained from (3.6) by replacement $C \to -|C|, \cos\phi = \cos 2\phi \to 1$. This energy should be minimized at a fixed total condensate density $n \equiv n_+ + n_- = n_0$ that is uniquely determined by the pumping power. The result depends on the sign of a simple combination of the energy constants $\Gamma = A - B + |C| - D$. At $\Gamma > 0$, the symmetric phase with $n_+ = n_-$ has minimal energy; at $\Gamma < 0$ the non-symmetric phase wins. The contrast of the interference pattern in the non-symmetric condensate state equals

$$\beta = \frac{4\sqrt{n_+ n_-}}{n + 2\sqrt{n_+ n_-}} = \frac{2|C|}{B - A + D + |C|}. \tag{3.7}$$

The dependence of β on magnetic field has a cusp singularity at the 0-π transition curve. It originates from the dependence of β on $|C|$, whereas C is a regular function of the field.

The values of the interaction coefficients can be approximately calculated using the Holstein-Primakoff approximation [4, 13, 15, 42, 43]. The calculations are similar to those described in the previous chapter, except that now fourth order terms in magnon operators need to be kept. We refer the reader to Eq. (1.9) in [42] for the explicit expressions of those coefficients (note that in our convention the coefficients in (3.5) are defined with an additional factor of 2 compared to theirs). Spin of the elementary cell in YIG is 20 at zero temperature and 14.5 at room temperature. Therefore, the Holstein-Primakoff approximation is valid with precision of roughly 10%. If calculated with this approximation coefficient A in thick films $d > 0.2$ μm is negative, and B is positive [15]. It means that the magnons belonging to the same condensate attract each other and repulse the magnons belonging to other condensate. If two other coefficients C and D would be zero, the condensate magnons would go to one of the minima leaving the second minimum empty. However, any non-zero value of C leads to emergence of nonzero condensate in the second minimum. It occurs because when the value of one of the condensate densities is low, the term with coefficient C in the condensate energy (6) is negative and large compared to the terms with coefficients B and D.

The state diagram found in [4] with coefficient C corrected according to Salman et al. [42] is shown in Fig. 3.2. The transitions from non-symmetric to symmetric state and from 0 to π-states can be observed in a given film at at varying magnetic field.

The two phases $\phi = \phi_+ + \phi_-$ and $\bar{\phi} = \phi_+ - \phi_-$ play very different roles in the condensate behavior. The first is trapped in quasi-equilibrium state by dipolar interaction. The second is a Goldstone mode. According to Eq. (3.2) it shifts the interference pattern as a whole with no change of energy. Its oscillations generate a sound-like collective excitation of the condensate called zero-sound [4].

3.4 Classical interpretation of magnon condensate

The BEC in cooled gases and in the liquid is definitely a quantum phenomenon. It proceeds when the thermal de Broglie wavelength assumes the same order of magnitude as the distance between particles. However, the condensate wave function becomes a classical field with both

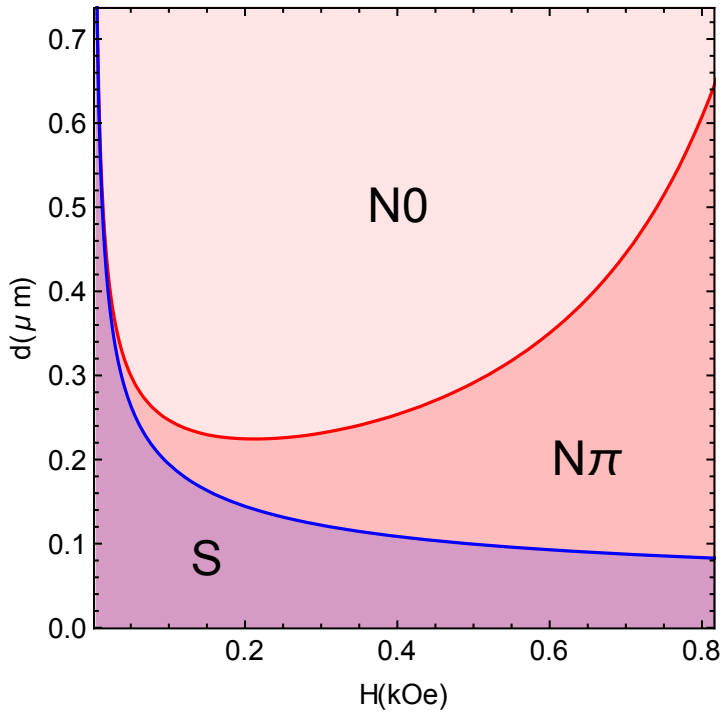

Figure 3.2: The state diagram in the d-H plane. S, $N0$ and $N\pi$ correspond to the symmetric state, the non-symmetric 0 state and the non-symmetric π state, respectively. The symmetric state is favorable at smaller d and H. The parameters are chosen as: $\gamma = 1.2 \times 10^{-5}$ eV/kOe, $\mathcal{D} = 0.24$ eVÅ^2, and $4\pi M = 1.78$ kOe.

the amplitude and phase simultaneously well defined. The condensation of magnons is a purely classical phenomenon. The condensate wave function is related to the local value of the complex transverse spin $S^+(\mathbf{x}) \equiv S^x(\mathbf{x}) + iS^y(\mathbf{x})$ by:

$$\psi(\mathbf{x}) = \frac{S^+(\mathbf{x})}{\sqrt{2Sv_0}}, \tag{3.8}$$

where v_0 is the volume of an elementary cell. Thus, the existence of condensate means the emergence of a macroscopic component of the total spin perpendicular to the average spin. Since there exists an external magnetic field along the average spin, this component rotates as a whole in time with angular velocity equal to $\Omega = \Delta/\hbar$. In the frame of reference rotating in the spin space with this angular velocity the order parameter $S^+(\mathbf{x})$ does not depend on time, but it is oscillating in space being a superposition of two plane waves as follows from eq. (3.1). The

transition to the rotating frame of reference is achieved by adding the term $-\mu N_c$ to the total condensate Hamiltonian, where N_c is total number of magnons in the condensate. In the presence of condensate $\mu = \Delta$.

Thus, it is possible in principle to solve the Landau-Lifshitz equation for magnetization, while avoiding any wave function. This is proposed by Rückriegel and Kopietz in the work [44]. However, we believe that the language of wave function and Bose-Einstein condensation is more adequate for this problem. The reason of the concentration of magnons at minima of the magnon energy is the same as in the conventional ideal or weakly interacting gas of Bose-Einstein particles: the finite "capacity" of the system in equilibrium. It means that, at a fixed temperature, the density of particles in Bose-Einstein gas cannot exceed a maximal value corresponding to chemical potential μ equal to the minimal energy of a particle. The wave function is a complex representation of the classical action-phase variables that lead to simplification of the mathematical structure of equations. The familiar idea of condensate, its flow and interference says more to physical intuition than a rather complicated picture of time-dependent magnetization.

To illustrate how the transition to condensate wave function simplifies the problem we demonstrate below magnetization corresponding to a simple condensate wave function of Eq. (3.2):

$$S^x = \sqrt{2Sv_0}\left[\sqrt{n_+}\cos\left(\mathbf{Q}\cdot\mathbf{x} - \Omega t + \phi_+\right) + \sqrt{n_-}\cos\left(\mathbf{Q}\cdot\mathbf{x} + \Omega t - \phi_-\right)\right], \tag{3.9}$$

$$S^y = \sqrt{2Sv_0}\left[\sqrt{n_+}\sin\left(\mathbf{Q}\cdot\mathbf{x} - \Omega t + \phi_+\right) - \sqrt{n_-}\sin\left(\mathbf{Q}\cdot\mathbf{x} + \Omega t - \phi_-\right)\right], \tag{3.10}$$

$$S^z = S - v_0\left[n_+ + n_- + 2\sqrt{n_+ n_-}\cos\left(2\mathbf{Q}\cdot\mathbf{x} + \bar{\phi}\right)\right]. \tag{3.11}$$

Eqs. (3.9-3.11) show the meaning of the phases $\phi_\pm$ in terms of the spin vector. The second term in Eq. (3.11) is square of length of the perpendicular component of magnetization. It independent of time, but is an oscillating function of coordinate x. The angle α between the perpendicular component of local spin and x-axis depends on coordinates and time:

$$\alpha(\mathbf{x},t) = -\arctan\frac{\sqrt{n_+}\sin\left(\mathbf{Q}\cdot\mathbf{x} - \Omega t + \phi_+\right) - \sqrt{n_-}\sin\left(\mathbf{Q}\cdot\mathbf{x} + \Omega t - \phi_-\right)}{\sqrt{n_+}\cos\left(\mathbf{Q}\cdot\mathbf{x} - \Omega t + \phi_+\right) + \sqrt{n_-}\cos\left(\mathbf{Q}\cdot\mathbf{x} + \Omega t - \phi_-\right)}. \tag{3.12}$$

The complex time dependence of the rotation angle is associated with the interference of the two condensates. If one of them, for example n_- becomes zero, the rotation proceeds with a constant angular velocity Ω independent of coordinates. The spin components in rotating frame of references $S^{x\prime} = S^x \cos\Omega t - S^y \sin\Omega t$ and $S^{y\prime} = S^x \sin\Omega t + S^y \cos\Omega t$ do not depend on time. The angle between this two-component vector and the x-axis is equal to

$$\alpha' = \arctan\left[\frac{\sqrt{n_+} \mp \sqrt{n_-}}{\sqrt{n_+} \pm \sqrt{n_-}} \tan(\mathbf{Q}\cdot\mathbf{x} + \phi_+)\right]. \tag{3.13}$$

In this equation we have employed the trapped phase ϕ. The upper signs correspond to $\phi = 0$, the lower signs correspond to $\phi = \pi$.

3.4.1 Discussions

We now discuss several other points:

1. The condensates of magnons observed in YIG is formed under external pumping, thus the condensate is formed not at equilbrium but at quasi-equilibrium. The the lifetime of magnons is much larger than the thermalization time between magnons, so that the system could reach a quasi-equibrium state for condensation to occur. This is quite different from the situation of BEC of cooled atoms – there the condensate is formed at equilibrium. Thus, there has been debates about whether the magnon condensate in YIG can indeed be called BEC [45]. But there will be no problem if one adopt that spontaneous coherence of quasiparticles is a defining characteristic of BEC. In [3] by observing the interference patterns between the two condensates, coherence of the magnons has been proved. Furthermore, in [46] it was shown that the coherence is not related to the coherent external pumping, thus it has to be spontaneous. With these observations, we believe that it is appropriate to call the magnon condensates in YIG "Bose-Einstein Condensates".

2. In this section when describing theoretically the formation of condensates we adopted a model in which all magnons has the same temperature and chemical potential. This was also the model used in the original experimental work [1]. In a later work [40] another model has been proposed to describe the formation of magnon condensates. The idea in [40] is that the external

pumping introduces a new energy scale, so that magnons are separated into two parts – the low-energy part which is directly influenced by pumping, and the high-energy part which is not directly influenced by pumping. Magnons in these two parts are taken to have different temperatures and chemical potentials: the high-energy part has room temperature and zero chemical potential, whereas the lower-energy part has a much higher temperature and chemical potential equal to the gap of the spectrum. Interactions between magnons in these two parts are governed by the so-called "evaporative supercooling" mechanism, which could be understood as similar to evaporation of liquid into gas, in which process heat is taken away from the remaining liquid so it is been cooled. Here because magnons in the lower-energy part have very high temperature, this cooling mechanism is very effective to lower the energies of these magnons (thus the name "supercooling"). This cooling from evaporation is responsible for the formation of condensates at the bottom of the lower-energy magnons. In [40] this model is used to explain their new experimental findings, but for our purpose the simpler model with a single temperature and chemical potential should be sufficient.

4. SUPERFLUIDITY OF MAGNONS IN FERROMAGNETIC FILMS*

BEC and superfluidity are closely related phenomena. Thus, natural questions arise for the BEC of magnons observed in YIG: can the magnon condensates behave like superfluid, and if so what are the properties of such magnon superfluid? Experimentally, observation of this superfluidity is still not realized. Currently there is only an indirect experimental evidence of magnon superfluidity in YIG reported by Bozhko et al. [47]. The authors observed relaxation of the condensate in a hot spot under the laser beam and stated that their series of curves could not be explained without non-zero supercurrent.

The possibility of superfluidity in a magnetic system was initially proposed by E.B. Sonin in 1978 [23]. His ideas regarding superfluidity in magnetic systems and in the exciton liquid in semiconductors are summarized in a review article [48] (Later we will make a detailed comparison between Sonin's work and our work). Several other theories were proposed in this century, most of them in the past 4 years. [49, 50, 51, 52, 53, 54]. Takei et al. [49] suggested to excite magnons in antiferromagnets. Takei and Tserkovniak [50], as well as Duine et al. [53], proposed to use electric current in metals to induce magnons with finite chemical potential in magnetic insulator like YIG. These are especially interesting since they relate to thin films and small samples, which are most important for potential technological applications.

In this chapter, we consider the possibility of superfluidity of condensed magnons in YIG. Starting with a Hamiltonian for magnon condensates, we will first derive and examine the equations of motion (EOMs) of the condensate amplitudes, and further for the condensate densities and phases. We then fix to the 1D stationary situation and show by calculations that the superfluidity of condensed magnons is indeed possible, and further that such superfluid has a rather unconventional

*Part of this chapter uses material with permission from "Unconventional superfluidity in yttrium iron Garnet films Physical review letters" by Chen Sun, Thomas Nattermann and Valery L. Pokrovsky, 2016, Physical Review Letters, 116, 257205, DOI: https://doi.org/10.1103/PhysRevLett.116.257205, Copyright 2016 by APS; and from "Bose-Einstein condensation and superfluidity of magnons in yttrium iron garnet films" by Chen Sun, Thomas Nattermann and Valery L. Pokrovsky, 2017, Journal of Physics D: Applied Physics, 2017, 50, 143002, Published 7 March 2017, DOI: https://doi.org/10.1088/1361-6463/aa5cfc, Copyright 2017 by IOP Publishing

behavior. For the calculations we will first use a variational method and an improved numerical shooting method. We also estimate the relative strength of superfluid and normal currents to show that the magnon superfluidity can indeed manifest itself, and discuss propose possible ways to achieve this superfluidity experimentally.

4.1 Model of superfluidity of magnons

4.1.1 Hamiltonian

Our starting point of calculation of superfluidity of magnons is based on the previously discussed theory of magnon condensates with fourth order interactions (3.5). We assume that the condensate amplitudes ψ_+ and ψ_- in (3.1) are slow functions of coordinates. For quadratic terms of the condensate amplitudes, we adopt the "effective mass approximation", so that total Hamiltonian for ψ_+ and ψ_- reads [4]:

$$\begin{aligned}\mathcal{H} = \int d^3x \Bigg[& \frac{1}{2m}\left(|\nabla\psi_+|^2 + |\nabla\psi_-|^2\right) - \mu\left(|\psi_+|^2 + |\psi_-|^2\right) \\ & + \frac{A}{2}\left(|\psi_+|^4 + |\psi_-|^4\right) + B|\psi_+|^2|\psi_-|^2 \\ & + \frac{C}{2}\left(|\psi_+|^2 + |\psi_-|^2\right)\left(\psi_+\psi_- + \psi_+^*\psi_-^*\right) + \frac{D}{2}\left(\psi_+^2\psi_-^2 + \psi_+^{*2}\psi_-^{*2}\right)\Bigg]. \end{aligned} \tag{4.1}$$

Here the $1/(2m)$ term is the effective mass term, and m is the effective mass of magnons at the spectrum minima along the direction of the external magnetic field. From the spectrum along this direction (2.70), we obtain $m = 1/(6\mathcal{D})$. The chemical potential μ is a Lagrangian factor ensuring the conservation of number of magnons in the condensate. This number is maintained constant by external microwave pumping. Correspondingly, the average density of condensed magnons n_0 is a constant. The meaning of the fourth order terms has been explained in the previous chapter in the paragraph after Eq. (3.5). Here we emphasize again that the C and D terms originate solely from the dipolar interaction, which does not conserve the number of magnons. We also note that generally $D \ll C$, thus in further considerations we will put $D = 0$.

4.1.2 Equations of motion

Starting from the Hamiltonian (4.1), let's write the equations of motions (EOMs) for condensate amplitudes $\psi_\pm$. This is achieved by taking functional differentiations $i\partial_t\psi_\pm = \delta\mathcal{H}/\delta\psi_\pm^*$:

$$i\partial_t\psi_+ = -3\mathcal{D}\nabla^2\psi_+ + \left(A\left|\psi_+\right|^2 + B\left|\psi_-\right|^2\right)\psi_+ + \frac{C}{2}\left[\psi_+^2\psi_- + \left(2\left|\psi_+\right|^2 + \left|\psi_-\right|^2\right)\psi_-^*\right] - \mu\psi_+, \tag{4.2}$$

$$i\partial_t\psi_- = -3\mathcal{D}\nabla^2\psi_- + \left(A\left|\psi_-\right|^2 + B\left|\psi_+\right|^2\right)\psi_- + \frac{C}{2}\left[\psi_-^2\psi_+ + \left(2\left|\psi_-\right|^2 + \left|\psi_+\right|^2\right)\psi_+^*\right] - \mu\psi_-. \tag{4.3}$$

Note that the EOMs of the amplitudes ψ_+ and ψ_- are related to each other by exchanging all subscripts $+$ and $-$. This is a direct consequence of the symmetry between the $+$ and $-$ condensates in the Hamiltonian (4.1). These two equations play the same role for the gas of magnons as the Gross-Pitaevskii equation for the gas of Bose-particles [55, 56].

The EOMs (4.2) and (4.3) can be rewritten in terms of the condensate densities $n_\pm$ and phases $\phi_\pm$ (recall that $\psi_\pm = \sqrt{n}_\pm e^{i\phi_\pm}$). We also define the currents as $\mathbf{j}_\pm = (n_\pm/m)\nabla\phi_\pm = 6\mathcal{D}n_\pm\nabla\phi_\pm$. Due to the complex nature of $\psi_\pm$, there will be 4 EOMs in terms of $n_\pm$ and $\phi_\pm$:

$$\partial_t n_+ + \nabla\cdot\mathbf{j}_+ = C(n_+ + n_-)\sqrt{n_+n_-}\sin(\phi_+ + \phi_-), \tag{4.4}$$

$$\partial_t\phi_+ = 3\mathcal{D}\left[\frac{\nabla^2 n_+}{2n_+} - (\nabla\phi_+)^2\right] - (An_+ + Bn_-) - \frac{C}{2}\left(3\sqrt{n_+n_-} + \frac{n_-^{\frac{3}{2}}}{\sqrt{n_+}}\right)\cos(\phi_+ + \phi_-) + \mu, \tag{4.5}$$

$$\partial_t n_- + \nabla\cdot\mathbf{j}_- = C(n_+ + n_-)\sqrt{n_+n_-}\sin(\phi_+ + \phi_-), \tag{4.6}$$

$$\partial_t\phi_- = 3\mathcal{D}\left[\frac{\nabla^2 n_-}{2n_+} - (\nabla\phi_-)^2\right] - (An_- + Bn_+) - \frac{C}{2}\left(3\sqrt{n_+n_-} + \frac{n_+^{\frac{3}{2}}}{\sqrt{n_-}}\right)\cos(\phi_+ + \phi_-) + \mu. \tag{4.7}$$

In light of the symmetry between $+$ and $-$, let's introduce the symmetric and antisymmetric

variables for these densities, phases and currents: $n = n_+ + n_-$, $\bar{n} = n_+ - n_-$, $\phi = \phi_+ + \phi_-$, $\bar{\phi} = \phi_+ - \phi_-$, $\mathbf{j} = \mathbf{j}_+ + \mathbf{j}_-$ and $\bar{\mathbf{j}} = \mathbf{j}_+ - \mathbf{j}_-$. The EOMs in terms of these new "symmetrized" variables read:

$$\partial_t n + \nabla \cdot \mathbf{j} = 2Cn\sqrt{n^2 - \bar{n}^2}\sin\phi, \tag{4.8}$$

$$\partial_t \bar{n} + \nabla \cdot \bar{\mathbf{j}} = 0, \tag{4.9}$$

$$\partial_t \phi = 3\mathcal{D}\sum_{\sigma=\pm}\left[\frac{\nabla^2\sqrt{n_\sigma}}{\sqrt{n_\sigma}} - (\nabla\phi_\sigma)^2\right] - (A+B)n - C\frac{(2n^2 - \bar{n}^2)\cos\phi}{\sqrt{n^2 - \bar{n}^2}} + 2\mu, \tag{4.10}$$

$$\partial_t \bar{\phi} = 3\mathcal{D}\left(\sum_{\sigma=\pm}\frac{\sigma\nabla^2\sqrt{n_\sigma}}{\sqrt{n_\sigma}} - \nabla\phi\nabla\bar{\phi}\right) - (A-B)\bar{n} + C\frac{n\bar{n}\cos\phi}{\sqrt{n^2 - \bar{n}^2}}. \tag{4.11}$$

We see that the first two equations are in the form of continuity equations. They demonstrate that the antisymmetric density $\bar{n}$ is a conserved value, whereas the local conservation of the total density is violated, due to the source term proportional to the coefficient C in the right-hand side of (4.8). The conservation of the antisymmetric current is a consequence of the symmetry of the Hamiltonian with respect to the free change of the Goldstone phase $\bar{\phi}$. The violation of the local conservation law for the total number of magnons in condensate is a consequence of the fact that dipolar interaction is non-invariant under the rotation in momentum space. It virtually turns the spin angular moment into the local rotation of the lattice and vice versa. This is why the local conservation is violated. However, globally the number of magnons may be conserved if the integral of the right-hand side of equation (4.8) is zero. Such opportunity may become regular due to the remnant symmetry of the Hamiltonian $\phi \leftrightarrow -\phi$. The dissipation due to rare decays and mergings with high-energy magnons is compensated by the pumping and does not introduce decoherence.

4.2 One-dimensional stationary superfluid flow

The EOMs (4.8-4.11) are too complicated to be solved exactly. Let's look at special cases to gain some physical insight. First, let's fix to the symmetric state, for which we have $n_+ = n_- = n/2$. We will also take $\phi_+ = \phi_- = \phi/2$. In this case $\bar{n} = \bar{\phi} = 0$, and the two equations for the

antisymmetric variables are trivially satisfied. The equations for the symmetric variables read:

$$\partial_t n + \nabla \cdot \mathbf{j} = 2Cn^2 \sin\phi, , \tag{4.12}$$

$$\partial_t \phi = 6\mathcal{D}\frac{\nabla^2\sqrt{n}}{\sqrt{n}} - \frac{3}{2}\mathcal{D}\left(\nabla\phi\right)^2 + (A+B)n - 2Cn\cos\phi + 2\mu. \tag{4.13}$$

If we further assume that n is a constant: $n = n_0$, then the continuity equation (4.12) becomes:

$$\frac{3\mathcal{D}}{2} n_0 \nabla^2\phi = 2Cn_0^2 \sin\phi, \tag{4.14}$$

or

$$\nabla^2\phi = \frac{4Cn_0}{3\mathcal{D}} \sin\phi. \tag{4.15}$$

If we further fix to the one-dimensional (1D) case, namely we assume that ϕ depends only on one spatial coordinate, then we recognize this equation as a sine-Gordon equation with no time dependence. Typical solutions of sine-Gordon equation are solitons. Solitons are structures where some quantity stays almost constant during large intervals but varies dramatically in a much smaller scale – the "soliton width". A periodic soliton structure is illustrated in Fig. 4.1.

For the actual system of equations (4.12) and (4.13), if we assume $n =$ const., then we would get only trivial solutions with $\phi =$ const. But it is reasonable to expect that this system of equations could still have nontrivial 1D solutions similar to solitons.

With this in mind, let's look at this 1D case in more detail. Consider a sample infinite in the direction parallel to the external field (or to the in-plane magnetization) that we define as the x-axis. This geometry is sketched in Fig. 4.2. (Note that previously we denote this direction to be the z-axis, but here since we are considering to the 1D case we will use the more natural spatial coordinate x.) We assume that condensate wave functions $\psi_\pm$ depend only on this coordinate x, not on other coordinates and on time. That is, we fix to the 1D stationary case. We will first consider the symmetric state, for which we have $n_+ = n_- = n/2$, and we assume $\phi_+ = \phi_- = \phi/2$. In this

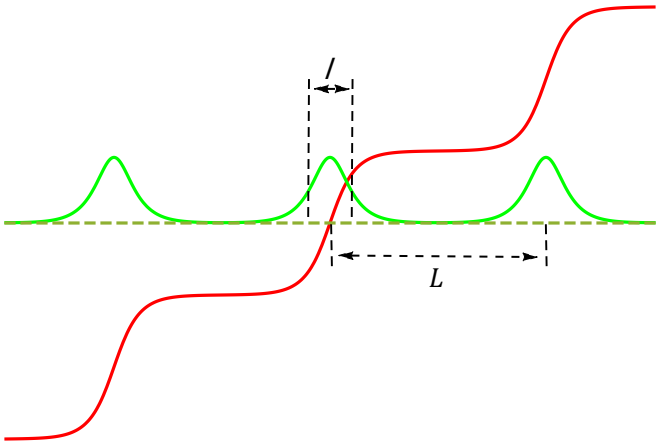

Figure 4.1: Illustration of phase (red) and superfluid velocity (green) of a periodic soliton structure in the approximation $n = \text{const}$. L is the period, ℓ is the soliton width. The velocity is proportional to the spatial derivative of the phase.

case, the Hamiltonian (4.1) reduces to:

$$\mathcal{H} = \mathcal{A} \int dx \left\{ \frac{\hbar^2}{8m} \left[\frac{1}{n} \left(\frac{dn}{dx} \right)^2 + n \left(\frac{d\phi}{dx} \right)^2 \right] + \frac{A+B}{4} n^2 + \frac{C}{2} n^2 \cos\phi - \mu n \right\}, \tag{4.16}$$

where $\mathcal{A}$ is the sample's cross section area perpendicular to the x direction. In obtaining this Hamiltonian we have written $\psi_\pm$ in terms of $n_\pm$ and $\phi_\pm$ and then used $n_+ = n_- = n/2$ and $\phi_+ = \phi_- = \phi/2$. Also we have dropped the D term.

We will look for a special class of solutions which are "quasiperiodic" with a period L. It means that the density n is a periodic function of x with the period L, whereas the phase ϕ is periodic by modulus 2π:

$$n(x+L) = n(x), \tag{4.17}$$

$$\phi(x+L) = \phi(x) + 2\pi. \tag{4.18}$$

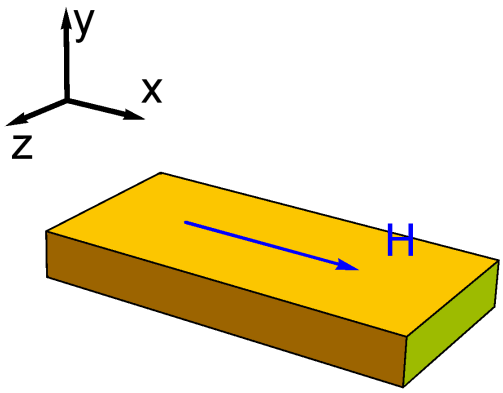

Figure 4.2: Geometry of the consideration for 1D case. The sample is infinite in the direction parallel to the external field $\mathbf{H}$, which is taken to be the x-axis.

The solutions should satisfy the condition of a fixed average density:

$$\frac{1}{L}\int_0^L n(x)dx = n_0. \tag{4.19}$$

We now scale the density n to be n/n_0, so that the average of density becomes 1. It is convenient to introduce a new unit of length, the "soliton width" ℓ:

$$\ell = \sqrt{3\mathcal{D}/(2\,|C|\,n_0)}. \tag{4.20}$$

We also scale x to be x/ℓ so that it becomes dimensionless. Plugging these new variables into the energy (4.16), we find the energy per unit volume in the unit $\sqrt{3|C|\mathcal{D}n_0^3/8}$:

$$\frac{\mathcal{H}}{V} = \frac{1}{L}\int_0^L dx\Big[\big(\frac{n'^2}{n} + n\phi'^2\big) + (\kappa + c\cos\phi)n^2 - \mu n - \mathcal{E}\Big]. \tag{4.21}$$

Here we introduced a new Lagrangian factor $\mathcal{E}$ to minimize at fixed change of ϕ per period, defined $c = \operatorname{sgn} c$, $\kappa = (A+B)/(2|C|)$, and scaled μ to be $(n_0|C|/2)\mu$. Prime denotes the derivative over x.

We further assume that ϕ is a monotonically growing function of x. Thus, we can introduce the

variable ϕ as argument instead of x. To solve the problem of stationary flow it is necessary to find periodic functions $n(\phi)$ and $f(\phi) \equiv (d\phi/dx)^2$ with period 2π that minimize the energy and obey the constraints of fixed averages:

$$\int_0^{2\pi} n(\phi)\frac{d\phi}{\sqrt{f(\phi)}} = \int_0^{2\pi} \frac{d\phi}{\sqrt{f(\phi)}} = L. \tag{4.22}$$

After we find such functions, the dependence $\phi(x)$ can be calculated by the inverse function:

$$x = \int_0^{\phi} \frac{d\phi}{\sqrt{f(\phi)}}. \tag{4.23}$$

The energy per unit volume (4.21) in this representation reads:

$$\frac{\mathcal{H}}{V} = \frac{1}{L}\int_0^{2\pi} \Big[\big(\frac{\dot{n}^2}{n} + n\big)f + (\kappa - \cos\phi)n^2 - \mu n - \mathcal{E}\Big]\frac{d\phi}{\sqrt{f}}, \tag{4.24}$$

where dots denote differentiation over ϕ, and we have we taken $C < 0$ for definiteness. Thus, now our problem is to find periodic functions $n(\phi)$ and $f(\phi)$ with period 2π that minimize the energy density (4.24) under constraints of fixed average density and spatial period (4.22).

We note that the Hamiltonian (4.24) as well as constraints (4.22) are invariant with respect to the reflection $\phi \to 2\pi - \phi$. Therefore the functions f and n corresponding to its energy minimum must be either even or odd. But being positive, these functions can not be odd. Thus, their Fourier expansions contain only $\cos m\phi$. This symmetry implies the global conservation law since it requires

$$\int_0^{2\pi} n^2 \sin\phi \frac{d\phi}{\sqrt{f(\phi)}} = \int_0^{L} n^2(x)\sin\left[\phi(x)\right] dx = 0. \tag{4.25}$$

Thus, integrating Eq. (4.8) over a period and employing parity of n, one finds that globally the number of particles in the condensate is conserved.

4.2.1 Variational method

To find the functions $n(\phi)$ and $f(\phi)$ in the energy density (4.24), we first employ a variational approach [6]. We approximate the functions $n(\phi)$ and $f(\phi)$ by Fourier-series truncated after the first two terms:

$$f(\phi) = f_0 - f_1 \cos\phi, \tag{4.26}$$

$$n(\phi) = n_0 + n_1 \cos\phi. \tag{4.27}$$

Since $n > 0$ and $f > 0$ for any ϕ, the 4 variational parameters f_0, f_1, n_0 and n_1 should satisfy $n_0 > |n_1|$ and $f_0 > |f_1|$.

4.2.1.1 Finite L – Periodic soliton structure

For any finite period L, we can use the two constraints (4.22) explicitly to eliminate 2 of the 4 parameters. In this case, the Lagrangian multiplier terms with μ and $\mathcal{E}$ in (4.24) are not necessary. Namely, we will minimize

$$\frac{\mathcal{H}}{V} = \frac{1}{L}\int_0^{2\pi} \Big[\big(\frac{\dot{n}^2}{n} + n\big) f + (\kappa - \cos\phi) n^2\Big] \frac{d\phi}{\sqrt{f}}, \tag{4.28}$$

under the constraints (4.22). (Note that we will use the same symbol $\mathcal{H}/V$ as in (4.24), although the μ and $\mathcal{E}$ terms are dropped.) The simplicity of the trial functions (4.26) and (4.27) allows us to perform analytically the integral in the variational Hamiltonian (4.28). The results are written in terms of complete elliptic integrals:

$$\begin{aligned}
\frac{\mathcal{H}}{V} = {} & \frac{4}{L\sqrt{\gamma-1}} \Bigg\{ \sqrt{f}_1 \Bigg[\frac{n_1^2 - n_0^2}{n_1} \left(\frac{n_0+\gamma n_1}{n_0+n_1} \Pi\left(\frac{2n_1}{n_0+n_1}, -\frac{2}{\gamma-1} \right) - K\left(-\frac{2}{\gamma-1} \right) \right) \\
& + 2n_0(\gamma-1) E\left(-\frac{2}{\gamma-1} \right) \Bigg] \\
& + \frac{1}{\sqrt{f}_1} \Bigg\{ \left[\kappa n_0^2 + (2\kappa n_0 n_1 - n_0^2)\gamma + \frac{1}{3}(\kappa n_1^2 - 2n_0 n_1)(2\gamma^2+1) - \frac{1}{15} n_1^2 \gamma (8\gamma^2+7) \right] K\left(-\frac{2}{\gamma-1} \right) \\
& - \left[(2\kappa n_0 n_1 - n_0^2) + \frac{2}{3}(\kappa n_1^2 - 2n_0 n_1)\gamma - \frac{1}{15} n_1^2 (8\gamma^2+9) \right] (\gamma-1) E\left(-\frac{2}{\gamma-1} \right) \Bigg\} \Bigg\},
\end{aligned} \tag{4.29}$$

where we have introduced the ratio

$$\gamma \equiv \frac{f_0}{f_1}, \tag{4.30}$$

and the $K(k)$, $E(k)$ and $\Pi(m,k)$ functions are the complete elliptic integrals of the first, the second and the third kind, respectively, defined as:

$$K(k) = \int_0^{\frac{\pi}{2}} \frac{d\theta}{\sqrt{1-k\sin^2\theta}}, \tag{4.31}$$

$$E(k) = \int_0^{\frac{\pi}{2}} d\theta \sqrt{1-k\sin^2\theta}, \tag{4.32}$$

$$\Pi(m,k) = \int_0^{\frac{\pi}{2}} \frac{d\theta}{(1-m\sin^2\theta)\sqrt{1-k\sin^2\theta}}. \tag{4.33}$$

We then use the constraints to eliminate 2 of the 4 parameters. Putting in the trial functions (4.26) and (4.27), the constraints (4.22) become:

$$\frac{4}{\sqrt{f_1(\gamma-1)}} K\left(-\frac{2}{\gamma-1}\right) = L, \tag{4.34}$$

$$n_0 + n_1\gamma - n_1(\gamma-1)\frac{E\left(-\frac{2}{\gamma-1}\right)}{K\left(-\frac{2}{\gamma-1}\right)} = 1. \tag{4.35}$$

From them we can express f_1 and n_0 in terms of γ and n_1:

$$\sqrt{f_1} = \frac{4K\left(-\frac{2}{\gamma-1}\right)}{L\sqrt{\gamma-1}}, \tag{4.36}$$

$$n_0 = 1 - n_1\left[\gamma - (\gamma-1)\frac{E\left(-\frac{2}{\gamma-1}\right)}{K\left(-\frac{2}{\gamma-1}\right)}\right]. \tag{4.37}$$

Plugging them into Eq. (4.29), we get the expression of the energy density $\mathcal{H}/V$ in terms of the 2 parameters γ and n_1. We then perform numerical minimization of $\mathcal{H}/V$ in (4.29) with respect to γ and n_1.

In Fig. 4.3 we show the dependences of the parameters (a) n_0 and n_1, (b) f_0 and (c) $\gamma = f_0/f_1$ on L at $\kappa = 2$. Fig. 4.3(d) demonstrates that at small L the amplitude f_0 grows as L^{-2}. Simultaneously the ratio $\gamma = f_0/f_1$ tends to ∞, and n_1/n_0 tends to zero approaching the standard superfluidity limit. In opposite limiting case of large L the ratio γ tends to 1, whereas f_0, n_0 and n_1 asymptotically approach to their single-soliton values (to be discussed later).

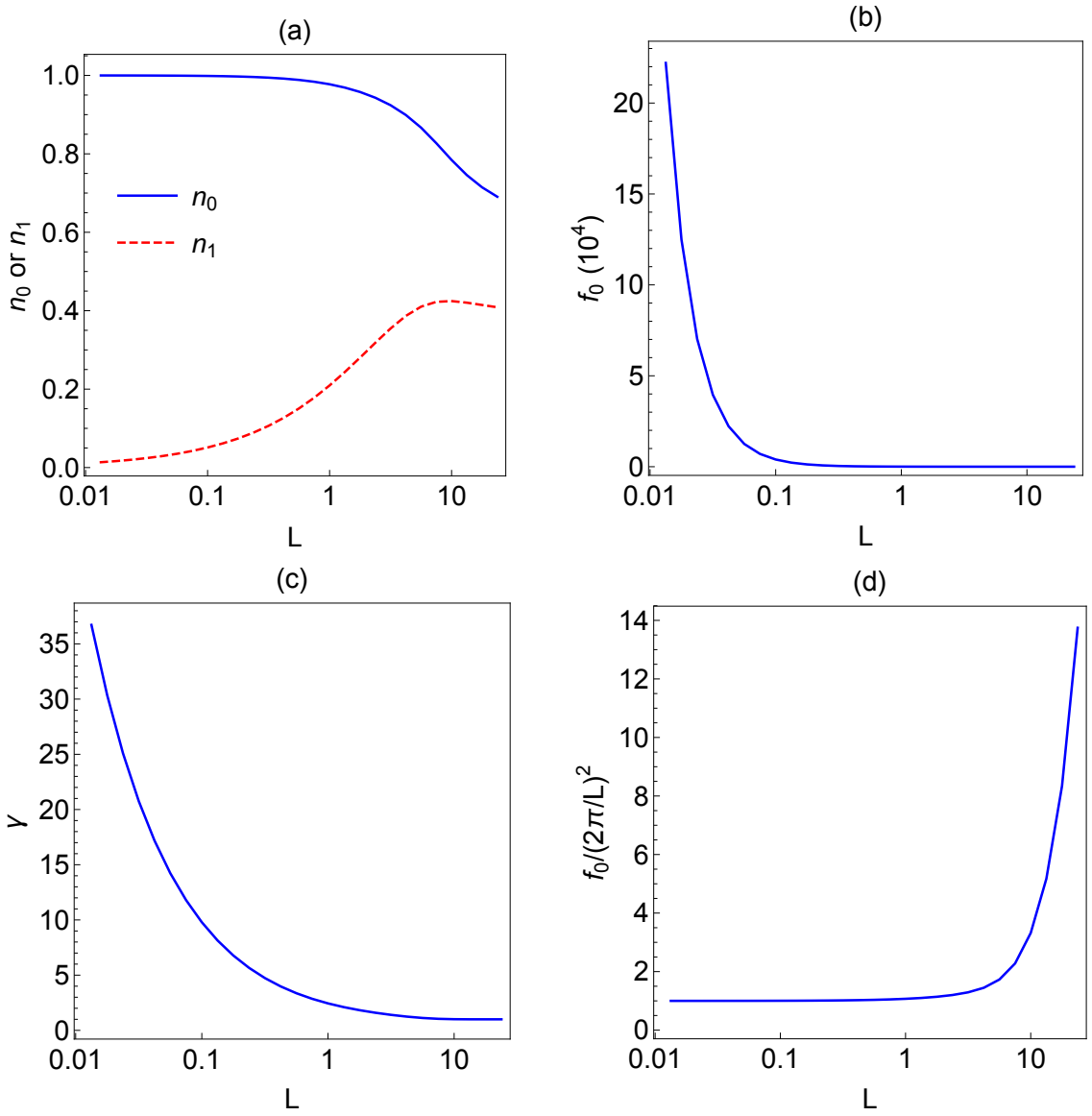

Figure 4.3: Dependence of the variational parameters on the period L in the symmetric phase at $\kappa = 2$: (a) n_0 and n_1; (b) f_0; (c) $\gamma = f_0/f_1$. In (d) the quantity $f_0/(2\pi/L)^2$ is plotted, which tends to 1 at small L.

Finally the dependence over coordinate x is restored by using (4.23). The results at different L's are shown in Figs. 4.4 and 4.5. In plots of Fig. 4.4 only one period is shown, whereas in the plots of Fig. 4.5 three periods are shown, which make the structures clearer. We see that at small L, the flow looks almost uniform where the phase ϕ increase uniformly and n slightly modulates around its average value. This is what we have in a traditional superfluid flow. However, at large L, the flow is non-uniform and "soliton-like": variations of both n and ϕ are confined to the "soliton" region; outside of this region, the angle stays near integer multiples of 2π. This is the effect of the $\cos\phi$ term in the Hamiltonian (4.28), which breaks the U(1) symmetry of rotation of the phase ϕ. Since minima of $-\cos\phi$ are at multiples of 2π, this term has the effect to trap the angle ϕ into multiples of 2π. Recalling that this cosine term comes from the C term which originates from the dipolar interaction, we can make an important observation that the dipolar interaction is responsible for such a soliton-like behavior of the superfluid flow. Physically, the number of magnons is not conserved locally in a stationary flow of the condensate. This non-conservation is associated with the transfer of spin moment to the lattice and with the inverse process induced by the dipolar interaction.

We note that starting from Eq. (4.24) we have assumed $C < 0$. The situation at $C > 0$ is similar, since it can be recovered by sending ϕ to $\phi + \pi$ in (4.24). In that case, the properties of the soliton-like motion will be the same, but the angle ϕ would prefer to stay at odd integer multiples of π instead of at integer multiples of 2π.

4.2.1.2 Infinite L – single-soliton case

Our previous calculations apply to any finite L. The $L \to \infty$ case, when there is a single soliton, requires special treatment. In this case, we expect that in $x \to \pm\infty$ we have $\phi = 0$ or 2π and $d\phi/dx = 0$. Thus, in the ϕ presentation, at $\phi = 0$ we should have $f = 0$. This indicates $f_0 = f_1$ for the 2-harmonics trial function (4.26). Besides, the constraints (4.22) reduces to:

$$\frac{\int_0^{2\pi} n(\phi)\frac{d\phi}{\sqrt{f(\phi)}}}{\int_0^{2\pi}\frac{d\phi}{\sqrt{f(\phi)}}} = 1. \tag{4.38}$$

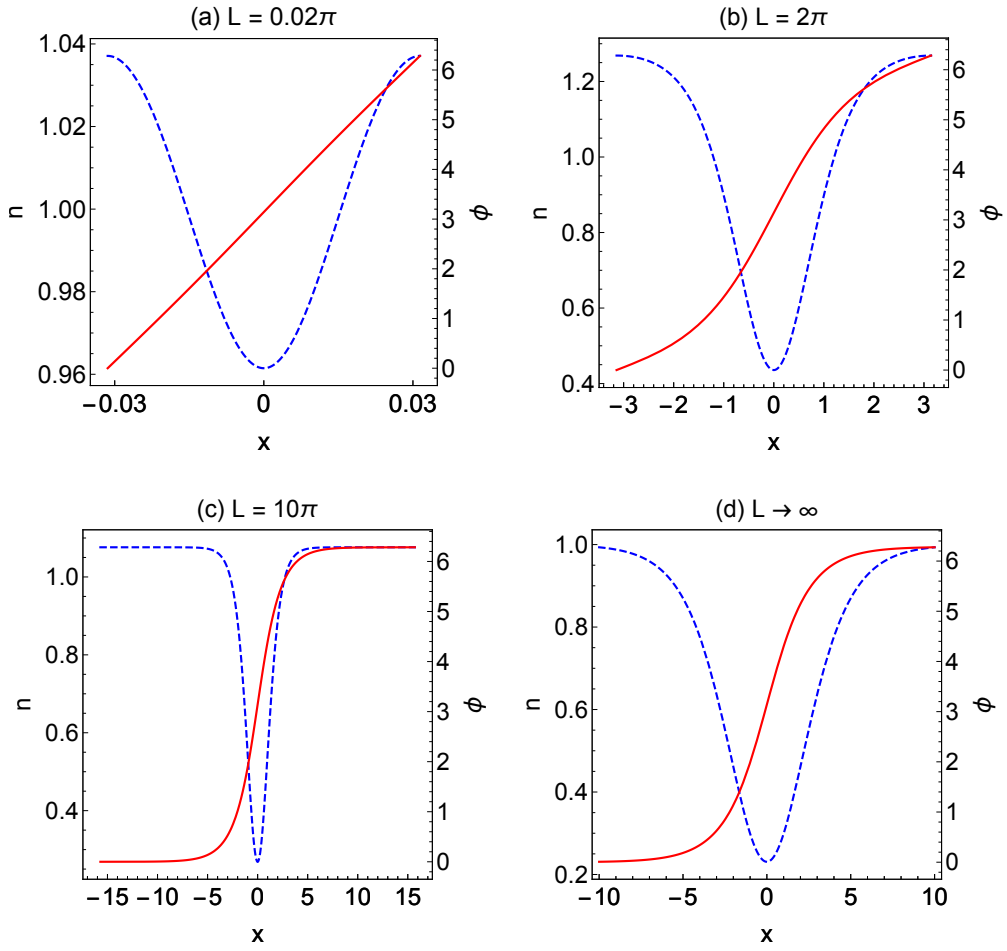

Figure 4.4: Variational solutions of the soliton structure in the symmetric state for different periods L, at $\kappa = 2$. The density n (blue, dashed curves) and the phase ϕ (red, solid curves) vs coordinate x are plotted within a single period L for: (a) $L = 0.02\pi$, (b) $L = 2\pi$, (c) $L = 10\pi$, (d) $L \to \infty$. In (d) a single soliton is shown in the range $x \in (-10, 10)$. The depth of modulation of the density and the phase decreases when L decreases. Note the different scales of n in different plots.

This equation is satisfied if we take $n = 1$ at $\phi = 0$, which implies $n_0 + n_1 = 1$. Thus, the 2-harmonics trial functions for the $L \to \infty$ case are

$$f(\phi) = f_0(1 - \cos\phi), \tag{4.39}$$

$$n(\phi) = 1 - n_1 + n_1 \cos\phi. \tag{4.40}$$

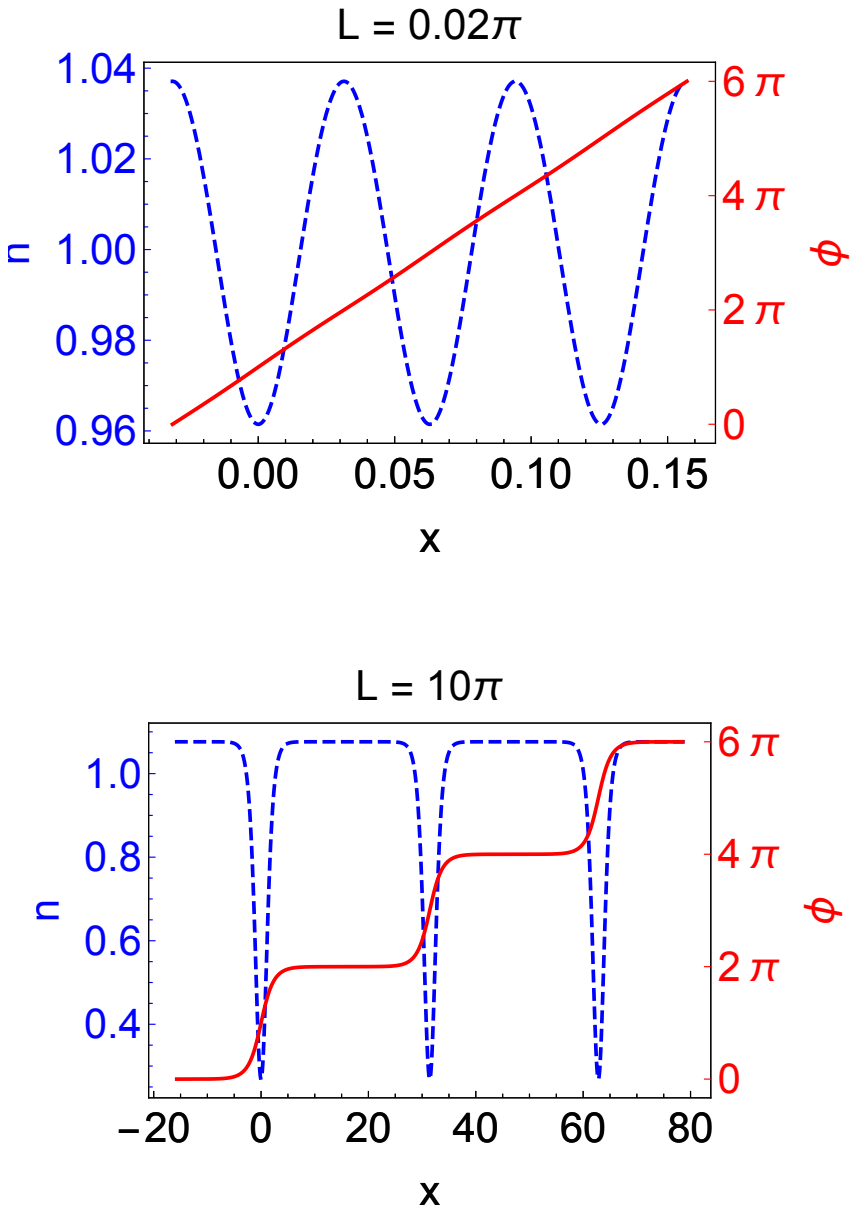

Figure 4.5: Variational solutions of the soliton structure in the symmetric state for different periods L, at $\kappa = 2$. The density n (blue, dashed curves) and the phase ϕ (red, solid curves) vs coordinate x are plotted within 3 periods for: (a) $L = 0.02\pi$; (b) $L = 10\pi$. Note the different scales of n in different plots.

The μ and $\mathcal{E}$ terms need to be included to make the integral of energy finite, because the integral of $(\kappa - \cos\phi)n^2/\sqrt{f}$ diverges. We choose μ and $\mathcal{E}$ to satisfy that $\partial_n[(\kappa - \cos\phi)n^2 - \mu n - \mathcal{E}] = 0$

and $(\kappa - \cos\phi)n^2 - \mu n - \mathcal{E} = 0$ at $\phi = 0$. These two conditions fix $\eta = 2(\kappa - 1)$ and $\mathcal{E} = \kappa - 1$. Performing the integrals in the (4.24), we get:

$$\frac{\mathcal{H}}{\mathcal{A}} = 4\left\{\sqrt{f_0}\left[2\sqrt{2}(1-n_1) - \sqrt{\frac{1-2n_1}{n_1}}\arcsin\sqrt{2n_1}\right] + \frac{\sqrt{2}}{\sqrt{f_0}}\left[1 - \frac{8}{3}n_1 + 4\left(\frac{1}{5} + \frac{\kappa}{3}\right)n_1^2\right]\right\}. \tag{4.41}$$

Note that in this case the energy is finite for infinite L, and the energy per unit volume $\mathcal{H}/V$ is zero. Thus, in Eq. (4.41) we have written the energy per unit area $\mathcal{H}/\mathcal{A}$ instead. We then numerically minimize (4.29) with respect to f_0 and n_1. The minimum for $\kappa = 2$ is at $f_0 = 0.7555$, $n_1 = 0.3846$, which in turn give $f_1 = 0.7555$, $n_0 = 0.6164$. In Fig. 4.3(a), we see that n_0 and n_1 at large L indeed approach to these single-soliton values. The observation in Fig. 4.3(c) that $\gamma \equiv f_0/f_1$ tends to 1 at large L is also consistent with the condition $f_0 = f_1$ as argued at the beginning of this section. Restoring the corresponding dependence on x, we find the single soliton structure, as illustrated in Fig. 4.4(d).

4.2.2 Shooting method

In the variational method discussed in the previous subsection, we were able to perform analytically the integration in the energy densities, which make the calculations convenient. However, since this method only includes 2-harmonics in the Fourier expansion, it does not claim for a high precision. Attempts to extend the length of truncated Fourier series lead to integrals which cannot be evaluated analytically. In this section, for the single-soliton case, we will use an advanced approach which reduces the two variational functions (f and n) to only one function. The price is a more complicated functional of energy that is not more a quadratic function of derivatives. Nevertheless, numerical calculation can still be performed.

The starting point of this approach is an observation that variational equation for function $f(\phi)$ has a simple explicit solution. Let's rewrite the Hamiltonian (4.24) in the form:

$$\frac{\mathcal{H}[n(\phi), f(\phi)]}{V} = \frac{1}{L}\int_0^{2\pi}\left(K\sqrt{f} + \frac{P}{\sqrt{f}}\right)d\phi, \tag{4.42}$$

where

$$K \equiv K\left(\dot{n}, n\right) = \frac{\dot{n}^2}{n} + n, \tag{4.43}$$

and

$$P \equiv P\left(n, \phi\right) = \left(\kappa - \cos\phi\right) n^2 - \mu n - \mathcal{E}. \tag{4.44}$$

Minimizing Eq. (4.42) over f, we find:

$$f = \frac{P}{K}. \tag{4.45}$$

Plugging this result into Eq. (4.42), we obtain the energy functional for the condensate density $n(x)$:

$$\frac{\mathcal{H}[n(\phi)]}{V} = \frac{2}{L}\int_0^{2\pi} \sqrt{KP} d\phi. \tag{4.46}$$

Equation of stationary flow following from Eq. (4.46) reads:

$$\frac{d}{d\phi}\left(\frac{\partial K}{\partial \dot{n}}\sqrt{\frac{P}{K}}\right) = \frac{\partial K}{\partial n}\sqrt{\frac{P}{K}} + \frac{\partial P}{\partial n}\sqrt{\frac{K}{P}}. \tag{4.47}$$

This equation can be solved numerically by the shooting method for the single-soliton case, namely when $L \to \infty$. In this case the constraints (4.22) must be replaced by boundary conditions:

$$n(0) = n(2\pi) = 1, \tag{4.48}$$

$$\dot{n}(\pi) = 0. \tag{4.49}$$

The value of chemical potential is the same as in the quasi-equilibrium state $\mu = 2(\kappa - 1)$. It was found by minimization of energy: $(\partial P/\partial n)|_{\phi=0} = 0$. Boundary conditions for the function f read $f(0) = f(2\pi) = 0$. Together with Eq. (4.45) it implies $P\big|_{\phi=0} = 0$ or equivalently $\mathcal{E} = \kappa - 1$. Thus, for a single soliton solution $P = (\kappa - 1)(n-1)^2 + \kappa n^2(1 - \cos\phi)$. At $\phi \to 0$, P approaches zero as ϕ^2. According to Eqs. (4.23) and (4.45), at $x \to \mp\infty$, the phase $\phi(x)$ asymptotically approaches 0 and 2π, respectively, as $e^{-\text{const.}|x|}$.

We solved Eq. (4.47) numerically by shooting from the point $\phi = \pi$ with zero derivative

and slowly change the value $n(\pi)$ until the boundary condition $n(0) = 1$ is satiefied. Fig. 4.6 shows several graphs of $n(\phi)$ for soliton solutions at different values of κ. The graphs of the same functions obtained by 2-harmonics variational method are also displayed in the same figure for comparison. They show that at $\kappa = 2$ and 3, the variational curve deviates from more precise shooting curve, though not dramatically. Their agreement becomes much better for $\kappa > 3$. We see that the variational approach is not too precise but works reasonably well for large enough κ ($\kappa > 3$). The shooting method becomes unstable and leads to unphysical singularities for $\kappa < 1$. This fact may be treated as an indication that the soliton solution does not exist in this range of κ, though we do not have a rigorous proof of this statement.

As compared to the variational method, the shooting method provides a more accurate treatment of the 1D superfluid flow problem. Still, there is no qualitative difference between the results of the two approaches. Especially, calculations by the shooting method confirms the soliton-like structure of the superfluid flow.

4.2.3 Stationary superfluid flow in the non-symmetric state

Let's now consider the non-symmetric state that according to the theory [4] emerges in thick films. In equilibrium the densities of the two condensates are different, i.e. $n_+ \neq n_-$. The stationary flow requires $\bar{\mathbf{j}}$ =const. Due to the larger number of variables, the calculation is more difficult. We found solution of this problem only for a special case $\bar{\mathbf{j}} = 0$. This relation allows to eliminate the variable $\bar{\phi}$ and obtain the effective Hamiltonian for remaining 3 variables:

$$\begin{aligned}\frac{\mathcal{H}}{V} = \frac{1}{L}\int dx \Bigg[& \frac{n_+'^2}{4n_+} + \frac{n_-'^2}{4n_-} + \frac{n_+ n_-}{n}\phi'^2 \\ & + \frac{a}{2}\left(n_+^2 + n_-^2\right) + b n_+ n_- - \sqrt{n_+ n_-}\, n \cos\phi - \mu n \Bigg],\end{aligned} \tag{4.50}$$

where $a = A/C$ and $b = B/C$. If ϕ is a monotonically growing function of x, it is possible to introduce the variable ϕ instead of x as argument as we did in previous section. After this change,

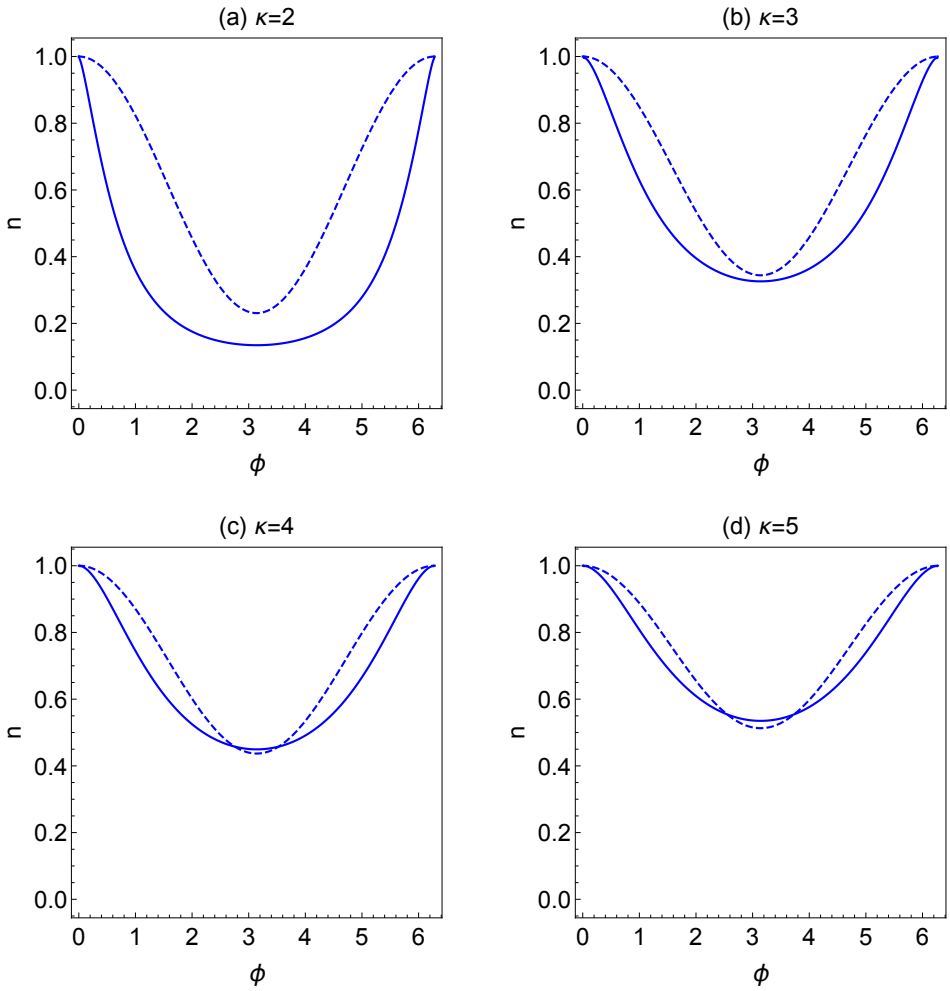

Figure 4.6: The condensate density n vs phase ϕ for different choices of κ's, for the single-soliton case ($L \to \infty$). The solid lines are generated by the shooting method, and the dashed lines are produced by the 2-harmonics variational method. The curves generated by the shooting method are more flat near $\phi = \pi$ compared to the variational result which includes only 2 harmonics. For $\kappa = 2$ the shooting method gives a considerably lower minimum value of n at $\phi = \pi$. Their agreement is better for $\kappa > 3$.

the energy (4.50) assumes a form:

$$\frac{\mathcal{H}}{V} = \frac{1}{L}\int_0^{2\pi} \left[\left(\frac{\dot{n}_+^2}{4n_+} + \frac{\dot{n}_-^2}{4n_-} + \frac{n_+ n_-}{n} \right) f \right. \\ \left. + \frac{a}{2}\left(n_+^2 + n_-^2\right) + b n_+ n_- - \sqrt{n_+ n_-}\, n \cos\phi - \mu n \right] \frac{d\phi}{\sqrt{f}}, \tag{4.51}$$

where we used the same notation $f \equiv (d\phi/dx)^2$. Minimizing energy (4.51) over f we find again that f is determined by Eq. (4.45) but with different K and P:

$$K = \frac{\dot{n}_+^2}{4n_+} + \frac{\dot{n}_-^2}{4n_-} + \frac{n_+ n_-}{n}, \tag{4.52}$$

$$P = \frac{a}{2}\left(n_+^2 + n_-^2\right) + b n_+ n_- - \sqrt{n_+ n_-}\, n \cos\phi - \mu n, \tag{4.53}$$

Thus, it is possible to eliminate f and get the Hamiltonian for the two densities n_+ and n_- that has the same form (4.46) but with different K and P defined by Eqs. (4.52) and (4.53). Minimization of this energy over n_+, n_- results in two differential equations. They must be solved with the constraints:

$$\int_0^{2\pi} n_\sigma \frac{d\phi}{\sqrt{f}} = \frac{1}{2}\Big(1 + \sigma\sqrt{1 - \frac{1}{(b-a)^2}}\Big), \qquad \sigma = \pm. \tag{4.54}$$

The shooting method for a system of two equations appears more difficult. Here, we perform the previously used variational calculation with two harmonics in each function solution for a single soliton. The result is shown in Fig. 4.7. They suggest that variation of density within a soliton in the non-symmetric state is much less than in symmetric one. This result has a simple explanation: in thick films the product $n_+ n_-$ is much less than n^2. It leads to a strong decrease of the coefficient at $\cos\phi$ in the Hamiltonian since $|C| n \sqrt{n_+ n_-} \approx |C|^2 n^2/(B - A)$. Thus, the coupling of phase to density is weakened by the factor $|C|/(B - A) \sim 1/Qd$. For a 5 μm thick film this factor is approximately 0.025.

4.2.4 Comparison with previous work

We have proposed that periodic soliton structures for superfluid flow can exist for BEC of magnons in YIG. The priority in finding periodic inhomogeneous soliton structure for superfluidity belongs to E.B. Sonin [23]. He has found it for easy-plane magnet (EPM) with a weaker in-plane anisotropy. The solitons in EPM emerge as a result of violation of the U(1) invariance exactly as in YIG. However, there are significant differences between the EPM and YIG. In the EPM the paramagnet-ferromagnet transition plays role of the BE condensation. In YIG the condensation

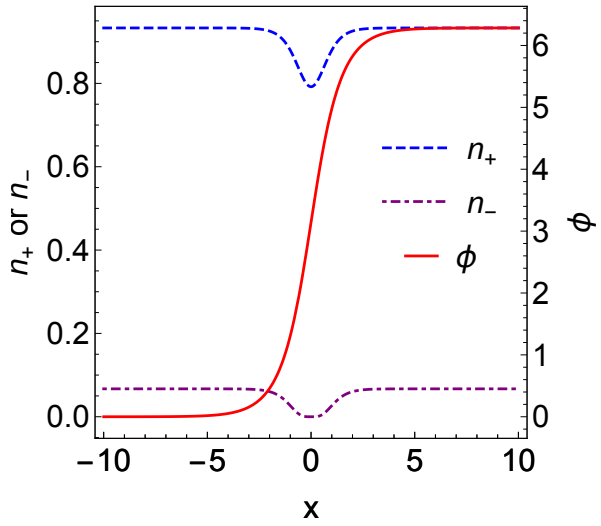

Figure 4.7: Variational single-soliton solution in the non-symmetric state at $a = 1$ and $b = 3$. Blue, dashed curve corresponds to n_+, purple, dot-dashed curve to n_+, and red, solid curve to ϕ.

is an independent transition at any temperature below the Curie point. The magnon BEC in the EPM is an equilibrium property (it is another name for the paramagnet-ferromagnet transition), whereas the BEC of magnons in YIG requires pumping. There is only one condensate in the EPM compared to two condensates in YIG-films. The superfluid flow in the EPM is a helical magnetic structure in which the total moment rotates around hard axis. This state is rather far from the ground state. It is not clear how it can be achieved starting from the homogeneous ground state. In YIG the moving condensate is a relatively small transverse perturbation of magnetization. The density of condensate (the absolute value of magnetization) remains constant in the superfluid flow in EPM, but as our calculation show, it varies significantly in YIG. In view of these differences, the existence of superfluid soliton structure in YIG does not follow from Sonin's theory. Our calculations show that indeed, the soliton structure does not exist in a range of parameter κ. It is also different in the symmetric and non-symmetric states.

4.3 Estimates of superfluid and normal currents

We have predicted the superfluidity of magnons in YIG, but there is an obstacle for this superfluidity to manifest itself – the dominance of the normal magnon density over the condensed magnon density. In the experiment [1], the density of condensed magnons is only $\sim 1\%$ of the density of normal magnons, and further increase of the condensate density is difficult. In this section, by estimating the relative strength of superfluid and normal currents, we show that the magnon superfluid, despite its much smaller density, can indeed manifest itself, since the strength of the superfluid current can be much larger than that of the normal current. (Note that there is another possible way to overcome the aforementioned obstacle: in an experimental setup when a short pulse of inhomogeneous magnetic field is applied to set the magnons in motion, after the magnetic field is switched off the normal flow relaxes after collision time, whereas the superfluid motion continues. Thus, it is possible for the superfluid flow to manifest itself in this situation.)

The spectrum of excitations in the magnet is determined in the rest frame of the crystal, i.e. in the lab frame. Therefore, the Landau criterion for superfluidity does not apply. Instead the critical velocity is determined as magnon velocity at which its decay into two magnons becomes possible. Since the kinetic energy strongly exceeds the interaction, the critical velocity is equal to the velocity of an excitation whose energy is equal to doubled energy gap $2\gamma H$. Thus, for the critical velocity we find $v_c = 2\sqrt{\mathcal{D}\gamma H}/\hbar \approx 0.42$ km/s. The excitation with this energy has wave vector q much larger than Q.

Another type of excitations is a vortex ring. We model it as a torus with the radius of central line R and the radius of transverse cross-section also R. The flow lines inside the torus are circles in planes perpendicular to the central line. Since the circulation of velocity is quantized in units h/m, the energy of the vortex ring is $E_v = 1/(2m)(nh)^2 R \ln(R/a)$ and its momentum is $p_v = \pi^2 \hbar n R^2$. The probability of fluctuation with such energy at room temperature becomes reasonably high at $R \leq 100$ nm. The critical velocity for excitation of such a vortex ring is $v_c = E_v/2p_v = (\hbar/mR)\ln(R/a) \approx 1$ km/s.

The condensate and the normal magnons are accelerated by the Stern-Gerlach force $\mathbf{F} =$

$g\mu_B s\nabla H$. Due to dipolar forces the spin of a magnon s is not exactly equal to 1, but the deviation is small in two important intervals of energy: in the vicinity of minimal energy and at magnon energy much higher than $4\pi\gamma M$ and γH. Under the action of Stern-Gerlach force thermal magnons with energy $\sim T$ perform diffusive drift motion with drift velocity $v_n = F\tau_n/m_n$, where τ_n is the collision time of thermal magnons and $m_n = \hbar^2/(2\mathcal{D})$ is their mass. The attenuation (level width) of a thermal magnon can be roughly estimated as T/S^2 which gives $\tau_n \sim 10^{-12}$ s at room temperature. Let the magnetic field to be generated by the current J flowing through a thin wire suspended over the YIG film at a distance equal to the width of the film w and parallel to its long side. Then the field gradient has the order of magnitude $J/(cw^2)$. Taking $J = 100$ mA and $w = 10$ μm, we find $|\nabla H| \approx 1$ T/cm and $F \approx 10^{-16}$ g·cm·s^{-2}. The drift velocity of normal magnons is $v_n \sim 1$ mm/s, 5-7 decimal orders of magnitude less than the superfluid critical velocity. However it is possible that the width of film is insufficient and the force can not accelerate the superfluid to its critical velocity. At fixed F, the length necessary to reach critical velocity is $l_c = mv_c^2/F$. At the same data $l_c = 1$ mm. It is larger than the width of the film in our example. Then the maximal velocity reached by the superfluid on the length w is $v_s = \sqrt{2Fw/m} \approx 100$ m/s, still by 5 orders of magnitude above the drift velocity. Thus, we realistically expect that the spin superfluid current equal to $10^{22} - 10^{23}$ cm^{-2}s^{-1} is by 3-5 decimal orders larger than the normal current. This justifies our consideration of the superfluid motion by itself, without any normal component, as we did in previous analysis.

4.4 Possible experiments to observe magnon superfluidity

Up to now, direct evidence of the existence of superfluidity of magnons in YIG has not been reported. In this section, we discuss possible ways to experimentally achieve and observe superfluidity.

To achieve superfluid flow in YIG is not a trivial problem since the magnons are confined within the sample. Stationary superfluid flow is possible in a film shaped as annulus with magnetic field directed along its central line. The superfluid flow in such a sample can be detected by measurement of the the Brilloin frequency shift: in a superfluid flow it changes by kinetic energy

of a condensate magnon in comparison to unmoving condensate.

An alternative approach is to excite a propagating non-linear wave in the condensate by applying a pulse of inhomogeneous magnetic field confined to a finite volume, for example by a superconducting ring or a wire. The emerging wave will propagate with a constant velocity determined by the energy transferred by the pulse. Such time-dependent flow can be registered by BLS.

The superfluid flow may influence spin injection into a metal contacting with the YIG film (usually Pt and Au are used) and the voltage bias in the metal induced by the inverse Spin-Hall effect [57]. The effect based on spin-torque mechanism is proportional to the spin current at the interface between the YIG film and metal. It can be strongly enhanced on the arrival of the condensate wave at the interface. This phenomenon may be important for technological applications.

The convective heat transfer similar to that in superfluid ^{4}He is hardly possible in magnon superfluids. The condensate density is very low compared to the total density of magnons. The gas of magnons as a whole is highly compressible. Therefore, the motion of a superfluid magnons causes only very weak counterflow of normal magnons. Consequently, the transfer of entropy is almost zero.

For the technological purposes and from the point of view of basic science it would be very useful to achieve the magnon BEC and superfluidity in small samples of YIG with the thickness 3-30 nm and other linear sizes between a few tens to 100 nm. This is technically quite challenging. The microstrip resonator cannot be applied since it is too big. Maximal size of the film can not be smaller than the magnon wavelength at minimum of magnon energy. In a thick film with $d = 5$ μm it is about 1 μm and it depends on thickness as $d^{1/3}$. The minimal possible thickness is the lattice constant 1.2 nm. The wavelength corresponding to this thickness is only 0.1 μm. However, it may be very different if other sizes of the sample also are small.

Detection of condensate in thin and small films cannot be realized by the BLS since an optical signal from such a small sample is very weak and optical wavelength becomes larger than the

size of sample. Instead the detection of condensate may be based on specific spectrum of the condensate oscillations.

Takei and Tserkovniak [49] and Duino et al. [53] proposed to apply electric current in adjacent thin layer of heavy metal Pt or Au to pump magnons into YIG film in the amount sufficient for appearance of the condensate. The idea is that in close proximity to the interface of the YIG film and an adjacent metal electron flopping its spin can excite a magnon. Energy and moment from electric current are transferred to the spin system due to Spin Hall effect. This idea is an attractive hypothesis since surface reactions are especially effective in thin samples. However, two features of these works make their relevance to YIG indirect. First, they use a simplified quadratic spectrum of magnons and thus miss all effects associated with the two condensates. More importantly, the electrons pump the magnons in a broad range of energy of the order of temperature and therefore only $1/100$ of them has a chance to relax to the condensate at magnetic field of the order 0.1 T.

4.5 Discussions

Discussions on several other issues are in order:

1. In the model we used to consider superfluidity of magnons, we made the effective mass approximation. But in reality this approximation may not be very accurate. Certainly, near each energy minimum there exists a range of quadratic dependence of energy on momentum. However, specifically in YIG this range is rather narrow. Until the quadratic approximation is valid, the same change of energy for the left and right minima corresponds to the same velocity of magnons in the two condensates. But if the quadratic approximation fails, the velocities of magnons in different condensates become different. For example, at magnetic field in the pulse by 30-40 Oe on the background of the permanent magnetic field 600 Oe, the ratio of the two velocities becomes equal to 2. Very soon such two condensates loose their coherence. It may lead to independent propagation of the two condensates at high velocities.

2. There is another problem – what does superfluidity mean if the pumping is necessary to support the condensate? In this respect our system is close to the laser. It may support a strong coherence at the cost of energy consumption. YIG film and laser are essentially different in the

character of the condensate state. In the case of laser the electromagnetic field plays the role of condensate. It is in the state very far from its ground state. Each photon of has energy very high compared to photon minimal energy and to the temperature of environment. In contrast to a laser, in YIG film the magnons in condensates have energy very close to minimal energy and much less than temperature.

3. Though the formation of magnon condensates and superfluidity requires pumping, the stability of the condensate at superfluid motion is warranted by the conservation laws that forbid reactions until the velocity reaches critical value. Therefore, it is reasonable to expect that once created superfluid motion will persist for a time interval long in comparison with intrinsic time scales without additional pumping.

5. CONCLUSIONS AND OPEN QUESTIONS

In this work, we considered superfluidity of magnons in ferromagnetic films. We predict that superfluid propagation in magnons is possible, and that it differs from superfluid motion in a usual bosonic sytem. The number of magnons is not conserved locally in a stationary flow of the condensate. This non-conservation is associated with the transfer of spin moment to the lattice and with the inverse process, which is mediated by the dipolar interaction. We looked especially at the 1D stationary case. We find that at low average superfluidity velocity the phase changes by 2π in the phase solitons and stays near its preferred values $2n\pi$ or $(2n+1)\,\pi$ on long intervals between solitons. The density also changes inside the solitons and is almost constant over the long intervals between them. This effect can possibly be observed by the BLS measurements. We demonstrated that in the developed flow the velocity of superfluid magnons is by several decimal orders larger than the velocity of normal magnons. As a consequence, the superfluid magnetic current strongly exceeds the normal current. We proposed several realizations of superfluid flow in the magnon liquid and the ways of its observation.

Below are some open questions which may worth further studies:

1. In our calculations to find the profile of superfluid flow, we applied shooting method to an infinite period L. It will be good to generalize the shooting method to the case of finite period L, but we haven't found ways to do so. The difficulty is that we don't know L in advance for each shooting calculation.

2. Our study has focused on the behavior of the static solitons of the magnon superfluid, i.e. the case when the superfluid density and phase do not depend on time. It is tempting to generalize the soliton solutions to the dynamic case when the solitons are moving. The shape of solitons should now depend on the moving velocity. For small velocities, we expect the shape to be close to that of the soliton, and perturbative methods could be useful. Calculations for the time-dependent are expected to be more complicated due to existence of the additional time variable.

3. In our calculations we assumed an ideal geometry which is infinite in one of the dimensions.

In reality materials must have boundaries. When a moving soliton reaches the end of a wire, we expect it to bounce back. It would be interesting to look at the behavior of a soliton at such a bouncing process, and find how its shape will change. This requires to study the dynamic generalization of solitons first.

4. In our model we include only interaction within magnons in the condensates, and assumed that the total number of condensed magnons is fixed. But the influence of normal fluid magnons on superfluid magnons may also be important. Thus, development of a more delicate model including the interactions from normal magnons would be useful. For this properties of normal magnons themselves are also needed, e.g. hydrodynamics of these magnons should be considered.

5. For the model it would also be nice to go beyond the effective mass approximation and take into account the asymmetry in the directions near each energy minimum in the magnon spectrum.

6. More extended directions on the study of magnon superfluidity could be: its excitation methods, its interaction with other systems (e.g. phonons), its possible applications to transferring information, ...

REFERENCES

[1] SO Demokritov, VE Demidov, O Dzyapko, GA Melkov, AA Serga, B Hillebrands, and AN Slavin. Bose–einstein condensation of quasi-equilibrium magnons at room temperature under pumping. *Nature*, 443(7110):430, 2006.

[2] RF W Damon and JR Eshbach. Magnetostatic modes of a ferromagnet slab. *Journal of Physics and Chemistry of Solids*, 19(3-4):308–320, 1961.

[3] P Nowik-Boltyk, O Dzyapko, VE Demidov, NG Berloff, and SO Demokritov. Spatially non-uniform ground state and quantized vortices in a two-component bose-einstein condensate of magnons. *Scientific reports*, 2:482, 2012.

[4] Fuxiang Li, Wayne M Saslow, and Valery L Pokrovsky. Phase diagram for magnon condensate in yttrium iron garnet film. *Scientific reports*, 3:1372, 2013.

[5] VV Kruglyak, SO Demokritov, and D Magnonics Grundler. J. of phys d. *Applied Physics*, 43:264001–264007, 2010.

[6] Chen Sun, Thomas Nattermann, and Valery L Pokrovsky. Unconventional superfluidity in yttrium iron garnet films. *Physical review letters*, 116(25):257205, 2016.

[7] Chen Sun, Thomas Nattermann, and Valery L Pokrovsky. Bose–einstein condensation and superfluidity of magnons in yttrium iron garnet films. *Journal of Physics D: Applied Physics*, 50(14):143002, 2017.

[8] Felix Bloch. Zur theorie des ferromagnetismus. *Zeitschrift für Physik*, 61(3-4):206–219, 1930.

[9] T Holstein and Hl Primakoff. Field dependence of the intrinsic domain magnetization of a ferromagnet. *Physical Review*, 58(12):1098, 1940.

[10] Freeman J Dyson. General theory of spin-wave interactions. *Physical review*, 102(5):1217, 1956.

[11] I Dzaloshinsky. A thermodynamic theory of ŚweakŠferromagnetism of antiferromagnets. *J. Phys. Chem. Solids*, 4:241, 1958.

[12] Tôru Moriya. New mechanism of anisotropic superexchange interaction. *Physical Review Letters*, 4(5):228, 1960.

[13] Sergio M Rezende. Theory of coherence in bose-einstein condensation phenomena in a microwave-driven interacting magnon gas. *Physical Review B*, 79(17):174411, 2009.

[14] NN Bogoliubov. On the theory of superfluidity. *J. Phys.(Ussr)*, 11:23, 1947.

[15] Fuxiang Li. *On the Magnon Bose Einstein Condensation in Ferromagnetic Film*. PhD thesis, 2014.

[16] VV Gann. Nonuniform resonance in a ferromagnetic plate. *SOVIET PHYSICS SOLID STATE, USSR*, 8(11):2537, 1967.

[17] RE De Wames and T Wolfram. Dipole-exchange spin waves in ferromagnetic films. *Journal of Applied Physics*, 41(3):987–993, 1970.

[18] T Wolfram and RE De Wames. Macroscopic and microscopic theories of dipole-exchange spin waves in thin films: Case of the missing surface states. *Physical Review Letters*, 24(26):1489, 1970.

[19] RE Arias. Spin-wave modes of ferromagnetic films. *Physical Review B*, 94(13):134408, 2016.

[20] BA Kalinikos. Excitation of propagating spin waves in ferromagnetic films. In *IEE Proceedings H (Microwaves, Optics and Antennas)*, volume 127, pages 4–10. IET, 1980.

[21] BA Kalinikos and AN Slavin. Theory of dipole-exchange spin wave spectrum for ferromagnetic films with mixed exchange boundary conditions. *Journal of Physics C: Solid State Physics*, 19(35):7013, 1986.

[22] Andreas Kreisel, Francesca Sauli, Lorenz Bartosch, and Peter Kopietz. Microscopic spin-wave theory for yttrium-iron garnet films. *The European Physical Journal B*, 71(1):59, 2009.

[23] EB Sonin. Phase fixation, excitonic and spin superfluidity of electron-hole pairs and antiferromagnetic chromium. *Solid State Communications*, 25(4):253–255, 1978.

[24] Gang Li, Chen Sun, Thomas Nattermann, and Valery L Pokrovsky. Long-wave magnons in a ferromagnetic film. *arXiv preprint arXiv:1710.05362*, 2017.

[25] LD Landau and EM Lifshitz. On the theory of the dispersion of magnetic permeability in ferromagnetic bodies. *Phy. Z. Sowjetunion*, 8:153, 1935.

[26] Amikam Aharoni. *Introduction to the Theory of Ferromagnetism*, volume 109. Clarendon Press, 2000.

[27] Pyotr Kapitza. Viscosity of liquid helium below the λ-point. *Nature*, 141(3558):74, 1938.

[28] JF Allen and AD Misener. Flow of liquid helium ii. *Nature*, 141(3558):75, 1938.

[29] Fritz London. On the bose-einstein condensation. *Physical Review*, 54(11):947, 1938.

[30] L Landau. Theory of the superfluidity of helium ii. *Physical Review*, 60(4):356, 1941.

[31] Mike H Anderson, Jason R Ensher, Michael R Matthews, Carl E Wieman, and Eric A Cornell. Observation of bose-einstein condensation in a dilute atomic vapor. *science*, 269(5221):198–201, 1995.

[32] Kendall B Davis, M-O Mewes, Michael R Andrews, NJ Van Druten, DS Durfee, DM Kurn, and Wolfgang Ketterle. Bose-einstein condensation in a gas of sodium atoms. *Physical review letters*, 75(22):3969, 1995.

[33] Michael Robin Matthews, Brian P Anderson, PC Haljan, DS Hall, CE Wieman, and Eric A Cornell. Vortices in a bose-einstein condensate. *Physical Review Letters*, 83(13):2498, 1999.

[34] Jacek Kasprzak, M Richard, S Kundermann, A Baas, P Jeambrun, JMJ Keeling, FM Marchetti, MH Szymańska, R Andre, JL Staehli, et al. Bose–einstein condensation of exciton polaritons. *Nature*, 443(7110):409, 2006.

[35] Jan Klaers, Julian Schmitt, Frank Vewinger, and Martin Weitz. Bose–einstein condensation of photons in an optical microcavity. *Nature*, 468(7323):545, 2010.

[36] Vladimir Cherepanov, Igor Kolokolov, and Victor L'vov. The saga of yig: spectra, thermodynamics, interaction and relaxation of magnons in a complex magnet. *Physics reports*, 229(3):81–144, 1993.

[37] CW Sandweg, MB Jungfleisch, VI Vasyuchka, AA Serga, P Clausen, H Schultheiss, B Hillebrands, A Kreisel, and P Kopietz. Wide-range wavevector selectivity of magnon gases in brillouin light scattering spectroscopy. *Review of Scientific Instruments*, 81(7):073902, 2010.

[38] AA Serga, CW Sandweg, VI Vasyuchka, MB Jungfleisch, B Hillebrands, A Kreisel, P Kopietz, and MP Kostylev. Brillouin light scattering spectroscopy of parametrically excited dipole-exchange magnons. *Physical Review B*, 86(13):134403, 2012.

[39] Yuriy M Bunkov and Grigory E Volovik. Bose-einstein condensation of magnons in superfluid 3 he. *Journal of Low Temperature Physics*, 150(3-4):135–144, 2008.

[40] Alexander A Serga, Vasil S Tiberkevich, Christian W Sandweg, Vitaliy I Vasyuchka, Dmytro A Bozhko, Andrii V Chumak, Timo Neumann, Björn Obry, Gennadii A Melkov, Andrei N Slavin, et al. Bose–einstein condensation in an ultra-hot gas of pumped magnons. *Nature communications*, 5:3452, 2014.

[41] VE Demidov, O Dzyapko, SO Demokritov, GA Melkov, and AN Slavin. Thermalization of a parametrically driven magnon gas leading to bose-einstein condensation. *Physical review letters*, 99(3):037205, 2007.

[42] Hayder Salman, Natalia G Berloff, and Sergej O Demokritov. Microscopic theory of bose–einstein condensation of magnons at room temperature. 2017.

[43] IS Tupitsyn, PCE Stamp, and AL Burin. Stability of bose-einstein condensates of hot magnons in yttrium iron garnet films. *Physical review letters*, 100(25):257202, 2008.

[44] Andreas Rückriegel and Peter Kopietz. Rayleigh-jeans condensation of pumped magnons in thin-film ferromagnets. *Physical review letters*, 115(15):157203, 2015.

[45] David Snoke. Condensed-matter physics: coherent questions. *Nature*, 443(7110):403, 2006.

[46] VE Demidov, O Dzyapko, SO Demokritov, GA Melkov, and AN Slavin. Observation of spontaneous coherence in bose-einstein condensate of magnons. *Physical review letters*, 100(4):047205, 2008.

[47] Dmytro A Bozhko, Alexander A Serga, Peter Clausen, Vitaliy I Vasyuchka, Frank Heussner, Gennadii A Melkov, Anna Pomyalov, Victor S LŠvov, and Burkard Hillebrands. Supercurrent in a room-temperature bose–einstein magnon condensate. *Nature Physics*, 12(11):1057, 2016.

[48] EB Sonin. Spin currents and spin superfluidity. *Advances in Physics*, 59(3):181–255, 2010.

[49] So Takei, Bertrand I Halperin, Amir Yacoby, and Yaroslav Tserkovnyak. Superfluid spin transport through antiferromagnetic insulators. *Physical Review B*, 90(9):094408, 2014.

[50] So Takei and Yaroslav Tserkovnyak. Superfluid spin transport through easy-plane ferromagnetic insulators. *Physical review letters*, 112(22):227201, 2014.

[51] Wei Chen and Manfred Sigrist. Spin superfluidity in coplanar multiferroics. *Physical Review B*, 89(2):024511, 2014.

[52] Kouki Nakata, Kevin A van Hoogdalem, Pascal Simon, and Daniel Loss. Josephson and persistent spin currents in bose-einstein condensates of magnons. *Physical Review B*, 90(14):144419, 2014.

[53] RA Duine, Arne Brataas, Scott A Bender, and Yaroslav Tserkovnyak. Spintronics and magnon bose-einstein condensation. *arXiv preprint arXiv:1505.01329*, 2015.

[54] Hans Skarsvåg, Cecilia Holmqvist, and Arne Brataas. Spin superfluidity and long-range transport in thin-film ferromagnets. *Physical review letters*, 115(23):237201, 2015.

[55] Eugene P Gross. Structure of a quantized vortex in boson systems. *Il Nuovo Cimento (1955-1965)*, 20(3):454–477, 1961.

[56] LP Pitaevskii. Vortex lines in an imperfect bose gas. *Sov. Phys. JETP*, 13(2):451–454, 1961.

[57] Yiyan Sun, Zihui Wang, and Lei Lu. Magnetic insulator-based spintronics: Spin pumping, magnetic proximity, spin hall, and spin seebeck effects on yttrium iron garnet thin films. In *Metallic Spintronic Devices*, pages 171–220. CRC Press, 2014.